© 2014. Published by The Company of Biologists Ltd | Development (2014) 141, 4254-4266 doi:10.1242/dev.115436

RESEARCH ARTICLE

STEM CELLS AND REGENERATION

SOX9 accelerates ESC differentiation to three germ layer lineages by repressing SOX2 expression through P21 (WAF1/CIP1)

Kohei Yamamizu[1], David Schlessinger[1] and Minoru S. H. Ko[1,2,*]

ABSTRACT

Upon removal of culture conditions that maintain an undifferentiated state, mouse embryonic stem cells (ESCs) differentiate into various cell types. Differentiation can be facilitated by forced expression of certain transcription factors (TFs), each of which can generally specify a particular developmental lineage. We previously established 137 mouse ESC lines, each of which carried a doxycycline-controllable TF. Among them, *Sox9* has unique capacity: its forced expression accelerates differentiation of mouse ESCs into cells of all three germ layers. With the additional use of specific culture conditions, overexpression of *Sox9* facilitated the generation of endothelial cells, hepatocytes and neurons from ESCs. Furthermore, *Sox9* action increases formation of *p21* (WAF1/CIP1), which then binds to the SRR2 enhancer of pluripotency marker *Sox2* and inhibits its expression. Knockdown of *p21* abolishes inhibition of *Sox2* and *Sox9*-accelerated differentiation, and reduction of *Sox2* 2 days after the beginning of ESC differentiation can comparably accelerate mouse ESC formation of cells of three germ layers. These data implicate the involvement of the *p21-Sox2* pathway in the mechanism of accelerated ESC differentiation by *Sox9* overexpression. The molecular cascade could be among the first steps to program ESC differentiation.

KEY WORDS: Embryonic stem cells, *Sox9*, *Sox2*, *Cdkn1a* (P21/WAF1/CIP1)

INTRODUCTION

The identity of cells can be altered by the forced induction of combination of transcription factors (TFs) (Takahashi and Yamanaka, 2006; Vierbuchen et al., 2010; Ieda et al., 2010; Sekiya and Suzuki, 2011; Huang et al., 2011; Hiramatsu et al., 2011), the forced induction of single TFs (Davis et al., 1987; Nishiyama et al., 2009; Correa-Cerro et al., 2011; Yamamizu et al., 2013) or by the repression of single TFs (Skarnes et al., 2004; Ivanova et al., 2006; Collins et al., 2007; Nishiyama et al., 2013). As an aid to analyze the effects of TF manipulation on mouse embryonic stem cell (ESC) differentiation, we have established the NIA Mouse ESC Bank (Nishiyama et al., 2009; Correa-Cerro et al., 2011), in which each of 137 TFs, i.e. 7-10% of all TFs encoded in the mouse genome (Kanamori et al., 2004), can be induced in a tetracycline-regulatable manner. We have measured the global gene expression profiles (i.e. transcriptome) of these ESC lines 48 h after overexpressing each TF (Correa-Cerro et al., 2011; Nishiyama et al., 2009). By comparing these transcriptome data to the publicly available expression profiles of a variety of cell types (Su et al., 2002; Wu et al., 2009), we generated a correlation matrix that can help to predict the TF-induced direction of ESC differentiation (Correa-Cerro et al., 2011). Based on predictions, we have successfully directed cell differentiation into target organ cells such as myocytes, hepatocytes, blood cells and neurons (Yamamizu et al., 2013).

Here, we have attempted an alternative use of the transcriptome data sets obtained by overexpressing each of 137 TFs in mouse ESCs. We selected the 36 ESC lines that individually showed the greatest degree of transcriptome perturbations and analyzed their early differentiation. As we expected, most TFs direct the ESC differentiation into cells ordinarily derived from one of the embryonic germ layers, but Sry (sex determining region Y) box 9 (SOX9), a member of the Sry-related high-mobility group (HMG) box transcription factors, is an exception. SOX9 had already been shown to have pivotal roles in embryonic development of multiple organs, including testis, chondrocytes, heart, lung, pancreas, bile duct, hair follicles, kidney, inner ear, retina and the central nervous system (Stolt et al., 2003; Chaboissier et al., 2004; Vidal et al., 2005; Akiyama et al., 2005; Seymour et al., 2007; Furuyama et al., 2011). Recent studies have shown that *Sox9* is expressed in progenitor cells of various organs and *Sox9*-expressing progenitors differentiate into multiple mature organ cells (Vidal et al., 2005; Seymour et al., 2007; Furuyama et al., 2011; Kadaja et al., 2014). However, molecular mechanisms for SOX9 function in progenitors are unclear. Here, we show that, in contrast to all other TFs tested, SOX9 can accelerate the differentiation of ESCs to cell types of all three germ layers. We have investigated the detailed molecular mechanism of this exceptional differential capacity of SOX9 in mediating ESC differentiation, and report the involvement of the *Cdkn1a* (P21/WAF1/CIP1)-*Sox2* pathway.

RESULTS

Identification of TFs that direct mouse ESC differentiation into three germ layers

Previously, we have reported global gene expression profiles of mouse ESC lines that were generated 48 h after overexpressing 137 TFs individually (Fig. 1A-C) (Nishiyama et al., 2009; Correa-Cerro et al., 2011). From a list of 137 TFs sorted by the magnitude of transcriptome perturbation, we arbitrarily selected the top 36 TFs (Fig. 1A-C) and analyzed systematically the differentiation into three germ layers using FACS, with FLK1, FOXA2 and PSA-NCAM as markers for mesoderm, endoderm and ectoderm, respectively. The ESC lines seemed to be differentiated into mixtures of cells of three germ layers, as these markers were not co-expressed in the same cells in most cases, according to the FACS and immunostaining analyses (supplementary material Fig. S1).

For mesoderm differentiation, overexpression of *T* (brachyury), which is known as a mesoderm inducer, increased the number of

[1]Laboratory of Genetics, National Institute on Aging, National Institutes of Health, Baltimore, MD 21224, USA. [2]Department of Systems Medicine, Sakaguchi Laboratory, Keio University School of Medicine, Tokyo 160-8582, Japan.

*Author for correspondence (kom@z7.keio.jp)

Received 15 July 2014; Accepted 4 September 2014

Development (2014) 141, 4254-4266 doi:10.1242/dev.115436

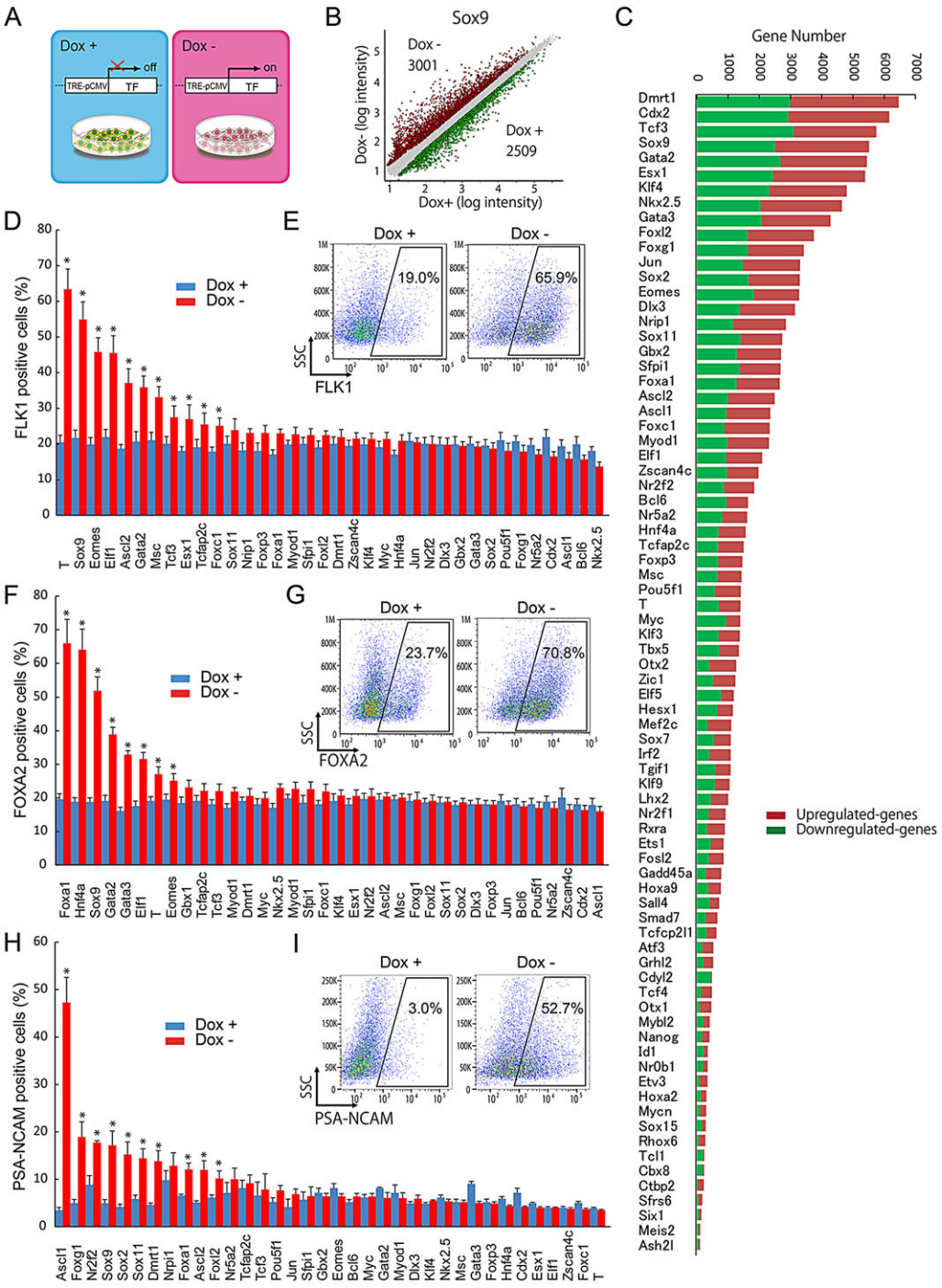

Fig. 1. Identification of TFs that efficiently differentiate ESCs into three germ layers by analyzing the NIA mouse ESC bank. (A) Schematic diagram of TF-inducible ESCs: each ESC line in the NIA mouse ESC bank contains one exogenous TF, the expression of which is repressed in the Dox+ condition, but induced in the Dox– condition. (B) Scatter-plot comparing gene expression profiles of SOX9-inducible ESC line cultured in Dox+ and Dox– conditions for 48 h. (C) The number of genes up- (red) and down- (green) regulated by the induction of TFs. (D) Thirty-six TFs ranked by the proportion of FLK1$^+$ cells measured by FACS analysis on day 5 of differentiation (three independent experiments; data are mean±s.e.m.; *P<0.05 versus Dox+). (E) An example of FACS analysis: appearance of FLK1$^+$ cells in ESCs carrying a *T* gene. (F) Thirty-six TFs ranked by the proportion of FOXA2$^+$ cells measured by FACS analysis on day 5 of differentiation (three independent experiments; data are mean±s.e.m.; *P<0.05 versus Dox+). (G) An example of FACS analysis: appearance of FOXA2$^+$ cells in ESCs carrying a *Foxa1* gene. (H) Thirty-six TFs ranked by the proportion of PSA-NCAM$^+$ cells measured by FACS analysis on day 5 of differentiation (three independent experiments; data are mean±s.e.m.; *P<0.05 versus Dox+). (I) An example of FACS analysis: appearance of PSA-NCAM+ cells in ESCs carrying a *Ascl1* gene.

FLK1-positive mesoderm cells most efficiently after 5 days of differentiation (Fig. 1D,E). *Sox9* is a second-ranked TF, the overexpression of which significantly increased the number of mesoderm cells from ESCs. Furthermore, we identified novel mesoderm inducers: *Ascl2*, *Tcf3*, *Esx1* and *Tcfap2* (*Tfap2e* – Mouse Genome Informatics). For endoderm differentiation, overexpression of *Hnf4a* and *Foxa1*, both of which are known as endoderm inducers, most efficiently increased the number of FOXA2-positive endoderm cells after 5 days of differentiation (Fig. 1F,G). *Sox9* is the third-ranked TF, the overexpression of which efficiently increased endoderm cells from ESCs. For ectoderm differentiation, overexpression of *Ascl1* most efficiently increased PSA-NCAM-positive ectoderm cells after 6 days of differentiation (Fig. 1H,I). *Sox9* is the fourth-ranked TF, the overexpression of which significantly increased the number of ectoderm cells from ESCs. These results indicate the utility of our approach to identify potent TFs such as *T*, *Hnf4a*, *Foxa1* and *Ascl1* for lineage-specific cell differentiation. Furthermore, among 36 ESC lines examined here, *Sox9* stood out as the only TF gene that ranked near the top of the list of genes necessary for the efficient differentiation of ESCs into all three germ layers.

Sox9 accelerates the differentiation of ESCs into three germ layers

Unique ability of SOX9 to efficiently direct differentiation into three germ layers prompted us to focus on *Sox9*. First, we confirmed *Sox9*

Development (2014) 141, 4254-4266 doi:10.1242/dev.115436

expression with qPCR and western blotting. In the control condition [doxycycline (Dox+)], endogenous *Sox9* levels increased from 3 days after differentiation (D3), preceding the emergence of the three germ layers (around D4) (Fig. 2A,B). By contrast, withdrawal of Dox on D0 increased the expression of exogenous *Sox9* from D1 (Fig. 2A,B). Immunostaining and FACS analyses showed that the Dox withdrawal on D0 markedly increased the proportion of cells expressing each of one of the three germ layer markers: FLK1 (KDR – Mouse Genome Informatics) and T (mesoderm); FOXA2 and SOX17 (endoderm); and NES (nestin) and PSA-NCAM (ectoderm) from D4 at comparable levels (Fig. 2C-G). Analyses by qPCR also showed that the forced overexpression of SOX9 increased the expression of mesoderm marker genes (*Flk1*, *T* and *Pdgfra*), endoderm marker genes (*Foxa2*, *Sox17* and *Gsc*) and ectoderm marker genes (*Nes* and *Fgf5*) from D2 or D3 (Fig. 2H). These results indicate that the forced expression of SOX9 in early differentiating cells regulates the generations of three germ layers from ESCs.

Sox9 enhances differentiation into endothelial cells, hepatocytes or neurons

To further examine ESC differentiation into organ cells, we used a lineage-specific medium with or without Dox from D3 to D7 (Fig. 3A). Under the control condition (Dox+), endothelial cells, hepatocytes and neurons did not appear even if cells were treated with lineage-specifying growth factors or cultured with lineage-specifying media (Yamamizu et al., 2012b, 2013). By contrast, the overexpression of *Sox9* combined with a treatment of vascular endothelial growth factor (VEGF) dramatically increased the proportion of endothelial cells stained with antibodies against CD31 and CDH5 (VE-Cadherin) by day 7 (Fig. 3B-D). Using hepatocyte-specific medium from D3, the overexpression of *Sox9* rapidly and dramatically increased the proportion of the hepatocytes, detected by the production of albumin (ALB) with immunostaining, by Periodic acid-Schiff (PAS) staining and by the uptake of low-density lipoproteins (LDL) (Fig. 3D). Furthermore, as early as D7, ALB production was detected in *Sox9*-overexpressing

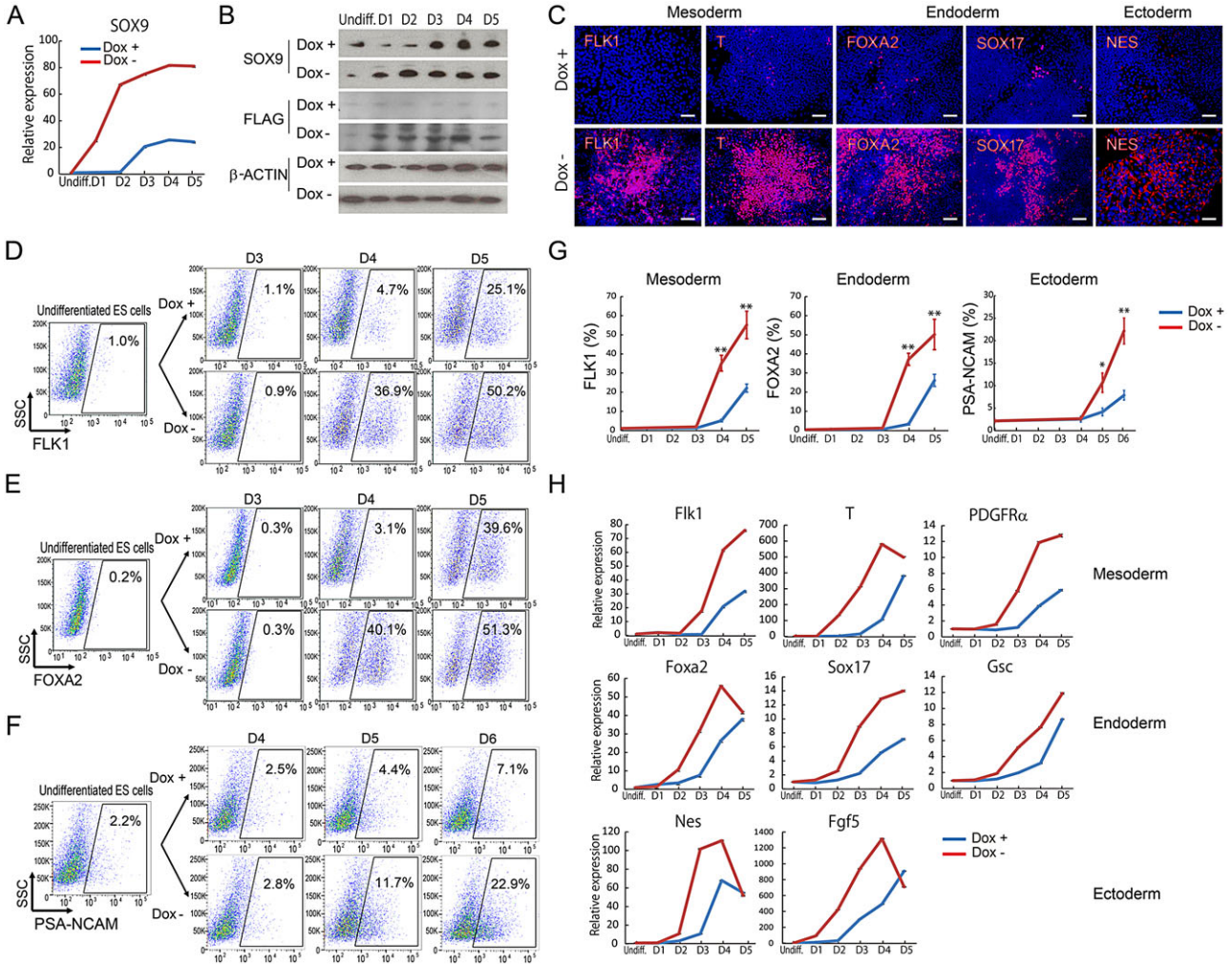

Fig. 2. Overexpression of *Sox9* enhances the differentiation of ESCs into three germ layers. (A) qPCR analysis showing the expression changes of *Sox9* (both endogenous and exogenous *Sox9*) during ESC differentiation. Blue line, Dox+; red line, Dox–. (B) Western blots detecting SOX9, FLAG and β-actin (control) during ESC differentiation in Dox+ or Dox– conditions. (C) Immunostaining of SOX9-inducible ESCs cultured for 4 days in Dox+ (control) or Dox– conditions: FLK1, T (mesoderm); FOXA2, SOX17 (endoderm); and NES (ectoderm). Scale bars: 200 µm. (D-F) Examples of FACS analyses for SOX9-inducible ESCs cultured for 3 days (D3), 4 days (D4), 5 days (D5) and 6 days (D6) in Dox+ (control) or Dox– conditions: detecting FLK1^{+} (D), FOXA2^{+} (E) or PSA-NCAM^{+} (F). (G) Summaries of three independent FACS experiments: blue line, Dox+; red line, Dox– (data are mean±s.e.m.; *P<0.05 versus Dox+). (H) qPCR analyses showing the expression changes of mesoderm marker genes (*Flk1*, *T* and *Pdgfra*), endoderm marker genes (*Foxa2*, *Sox17* and *Gsc*) and ectoderm marker genes (*Nes* and *Fgf5*) during ESC differentiation. Blue line, Dox+; red line, Dox–.

Development (2014) 141, 4254-4266 doi:10.1242/dev.115436

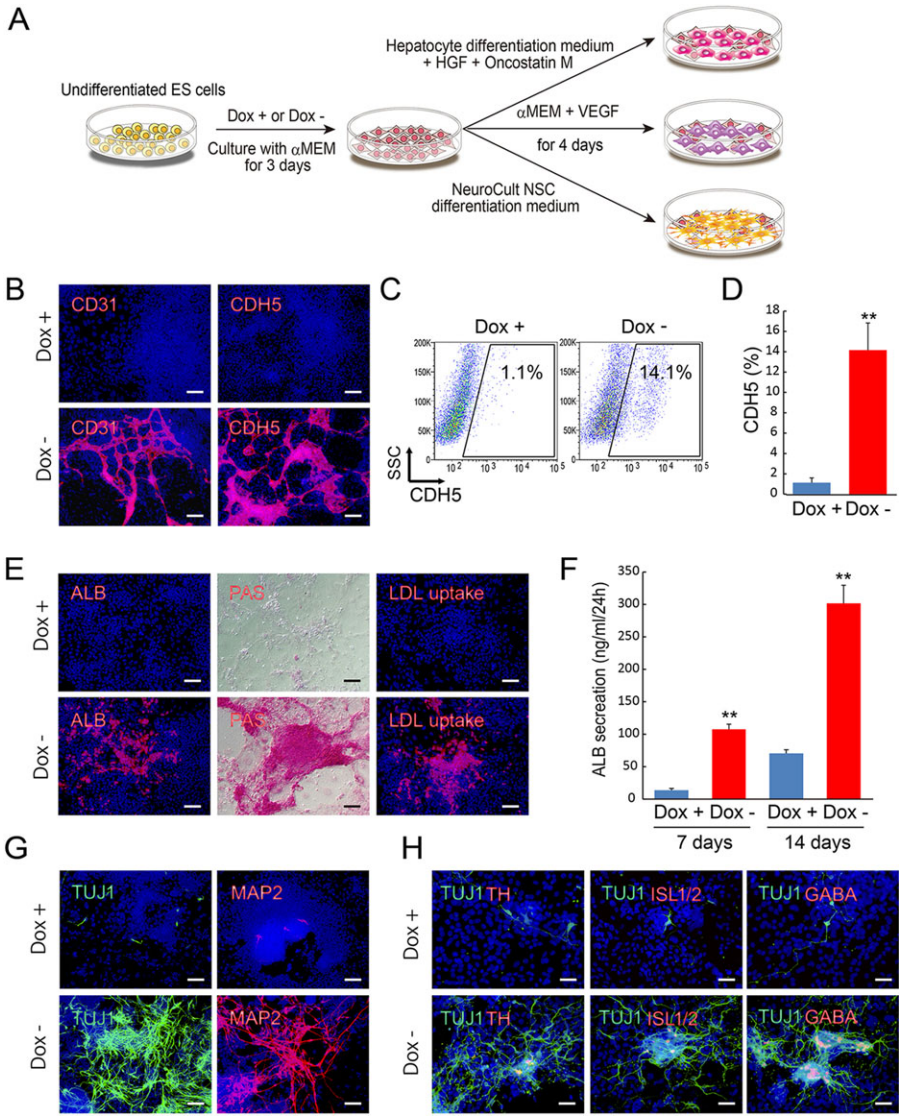

Fig. 3. Overexpression of *Sox9* enhances the differentiation of ESCs into endothelial cells, hepatocytes or neurons. (A) Schematic representation of experimental designs. (B) Immunostaining of SOX9-inducible ESCs cultured for 7 days in Dox+ (control) or Dox– conditions: endothelial cell markers, CD31 and CDH5 (VE-cadherin). Scale bars: 200 µm. (C) Examples of FACS analyses for SOX9-inducible ESCs cultured for 7 days in Dox+ (control) or Dox– conditions: detecting $CDH5^{+}$ endothelial cells. (D) A summary of three independent FACS experiments (data are mean±s.e.m.; $^{**}P<0.01$ versus Dox+). (E) Analyses of SOX9-inducible ESCs cultured for 7 days in Dox+ (control) or Dox– conditions: immunostaining of ALB, PAS staining and LDL uptake. Scale bars: 200 µm. (F) Amounts of ALB produced in the culture media from Sox-inducible ESCs, measured on D7 and D14 (three independent experiments; data are mean±s.e.m.; $^{**}P<0.01$ versus Dox+). (G,H) Immunostaining of SOX9-inducible ESCs cultured for 7 days in Dox+ (control) or Dox– conditions: TUJ1, MAP2, TH, ISL1/2 or GABA. Scale bars: 200 µm.

cells, but not in the Dox+ control cells, which became more prominent by D14 (Fig. 3E). Use of neuron-specific medium increased the *Sox9*-mediated efficiency of neural differentiation (Fig. 3G). Neurons induced by *Sox9* expressed a variety of neural markers: pan-neural markers (TUJ1 and MAP2); a dopaminergic neuron marker [tyrosine hydroxylase (TH)]; a motor neuron marker (ISL1/ISL2); and an inhibitory neurotransmitter (GABA) (Fig. 3H). Taken together, *Sox9* accelerates the differentiation of ESCs into progenitors of the three germ layers, thereby enhancing generation of organ cells.

Sox9 decreases pluripotent markers in early differentiating ESCs

Next, we examined markers of undifferentiated ESCs during differentiation induced by the overexpression of *Sox9*. Under the control condition (Dox+), alkaline phosphatase (AP)-negative differentiated colonies appeared from D5. By contrast, the overexpression of *Sox9* (Dox−) induced the appearance of AP-negative colonies from D4 (Fig. 4A,B). FACS analysis for a pluripotent marker, SSEA1, revealed that the overexpression of *Sox9* significantly decreased SSEA1-positive undifferentiated cells from D3 (Fig. 4C,D). Immunostaining and qPCR analyses for pluripotent markers – POU5F1, NANOG, SOX2 and SSEA1 – also revealed an earlier disappearance of these proteins, when *Sox9* is overexpressed. These results suggest that *Sox9* could be involved in the reduction of pluripotency that occurs during ESC differentiation.

Blocking endogenous *Sox9* activation inhibits the differentiation into three germ layers and maintains pluripotent markers in early differentiating ESCs

To investigate roles of endogenous *Sox9* in early differentiating ESCs, we blocked *Sox9* expression by treating cells with an siRNA against *Sox9*. As shown in Fig. 2B, endogenous *Sox9* increased from D3, preceding the emergence of the three germ layers (around D4) (Fig. 2B). We treated cells with three independent siRNAs against *Sox9* from D0 (Fig. 5; supplementary material Fig. S2). Analyses by FACS, immunostaining and qPCR clearly showed that the treatment with siRNAs against *Sox9* significantly inhibited the expression of mesoderm markers (FLK1, T and PDGFRα), endoderm markers (FOXA2, SOX17 and GSC) and ectoderm markers (NES and FGF5). Furthermore, treating cells with siRNAs against SOX9 maintained the expression of pluripotency markers (SSEA1, POU5F1, NANOG and SOX2), which are otherwise downregulated, in early differentiating ESCs (Fig. 5C-O; supplementary material Fig. S2B,C). These results

Development (2014) 141, 4254-4266 doi:10.1242/dev.115436

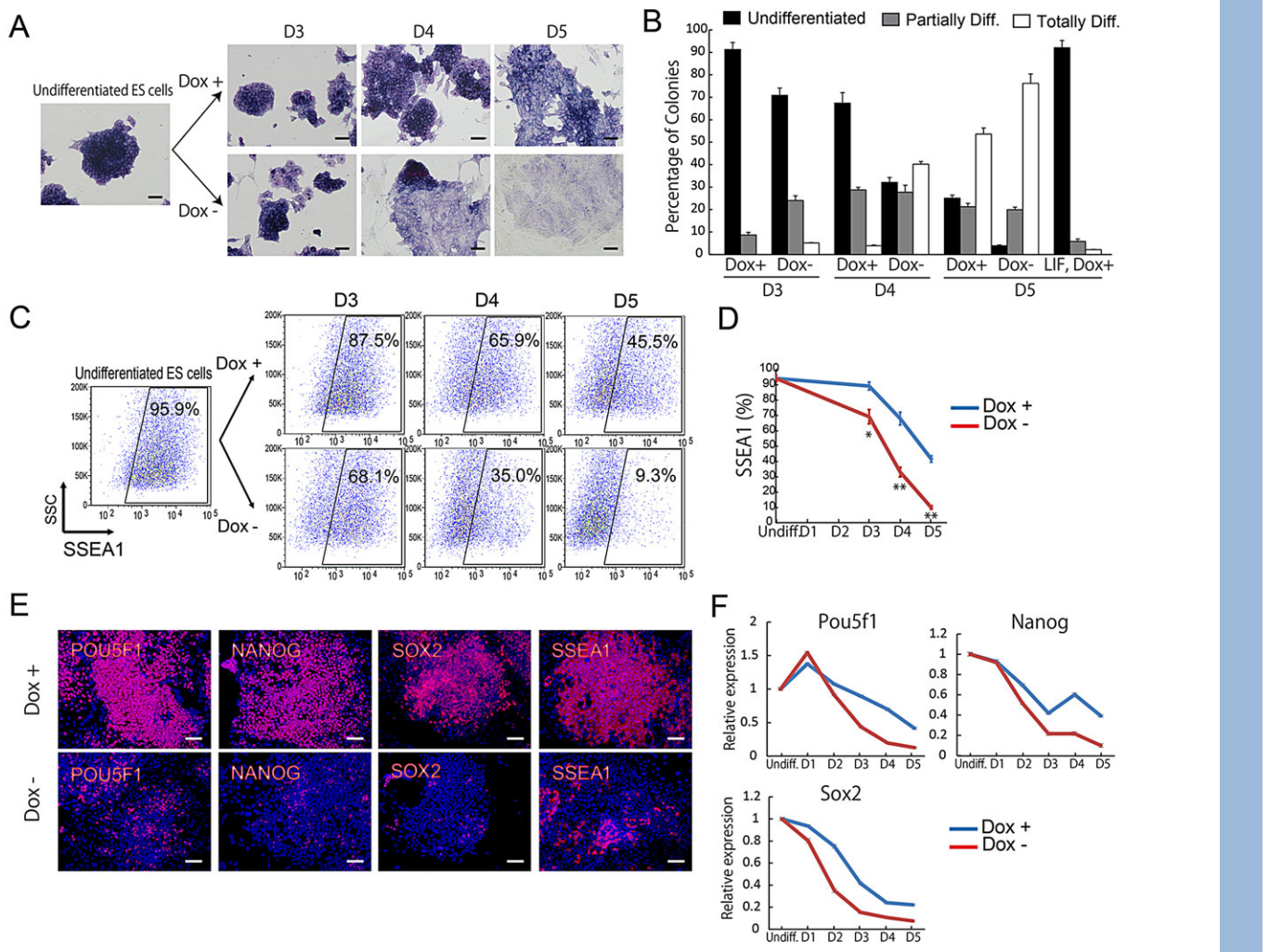

Fig. 4. Overexpression of *Sox9* decreases the expression of pluripotency markers in early differentiating ESCs. (A) Representative microscopic images of SOX9-inducible ESCs stained with alkaline phosphatase (AP) after culturing in Dox+ (control: upper panel) or Dox– (lower panel) for 3 (D3), 4 (D4) and 5 days (D5). Scale bars: 100 µm. (B) Morphometric analyses of AP-stained colonies (three independent experiments). (C) Examples of FACS analyses: SOX9-inducible ESCs stained for SSEA1^{+} after culturing in Dox+ (control: upper panel) or Dox– (lower panel) conditions for 3 (D3), 4 (D4) and 5 days (D5). (D) A summary of three independent FACS experiments (data are mean±s.e.m.; **P*<0.05 and ***P*<0.01 versus Dox+). (E) Representative microscopic images of SOX9-inducible ESCs immunostained for POU5F1, NANOG, SOX2 and SSEA1 after culturing in Dox+ (control: upper panel) or Dox– (lower panel) conditions for 4 days. Scale bars: 200 µm. (F) qPCR analyses showing the expression changes of pluripotency markers (*Pou5f1*, *Nanog* and *Sox2*). Blue line, Dox+; red line, Dox–.

indicate that the expression of endogenous SOX9 in early differentiating cells is required for both the generation of three germ layers from ESCs and the repression of pluripotency.

p21 (WAF1/CIP1) induced by *Sox9* represses *Sox2* expression through direct binding to an SRR2 enhancer

As proliferation and differentiation are considered to be closely related to each other, we examined cell proliferation during SOX9-induced ESC differentiation. The overexpression of *Sox9* significantly decreased cell numbers from D3 (Fig. 6A). FACS analysis also revealed that the cell population in G1 phase increased by *Sox9* overexpression from D2 (Fig. 6B; supplementary material Fig. S3). Previous studies have shown that, although pluripotency is associated with a specific cell-cycle profile characterized by a shortened G1 phase, pluripotent stem cells exhibit a lengthening of the G1 phase during differentiation produced by G1-checkpoint genes, such as *p21* and *p27* (Becker et al., 2006; Egozi et al., 2007). Accordingly, we investigated the expression of genes related to the G1 phase. We found that in the Dox– condition (i.e. the overexpression of *Sox9*), the level of *p21* was markedly increased from D2, whereas in the Dox+ condition (control), the level of *p21* was increased from D4 (Fig. 6C). The increase in *p21* levels from D4 is most likely caused by the upregulation of endogenous SOX9 expression from D3 (Fig. 2A), because blocking the activation of endogenous *Sox9* with an siRNA against *Sox9* inhibited the increase of *p21* expression that normally occurs from D4 (supplementary material Fig. S4). The expression levels of *p27*, but not of *p53* or *Rb*, were slightly increased by the overexpression of *Sox9*.

Western blotting analysis revealed an early increase of P21 and a reciprocal decrease of SOX2 levels from D2 caused by the overexpression of *Sox9* (Fig. 6D,E). Decreases in levels of POU5F1 and NANOG occurred later than the decrease in the levels of SOX2. It has been shown that P21 can modulate transcription by directly binding to specific promoters in a cell cycle-independent manner (Devgan et al., 2005; Besson et al., 2008). A recent study has shown that P21 directly binds to a *Sox2* enhancer and negatively regulates *Sox2* expression in neural stem cells (Marqués-Torrejon et al., 2013). The main regulatory element, named SRR2, that is responsible for the

Development (2014) 141, 4254-4266 doi:10.1242/dev.115436

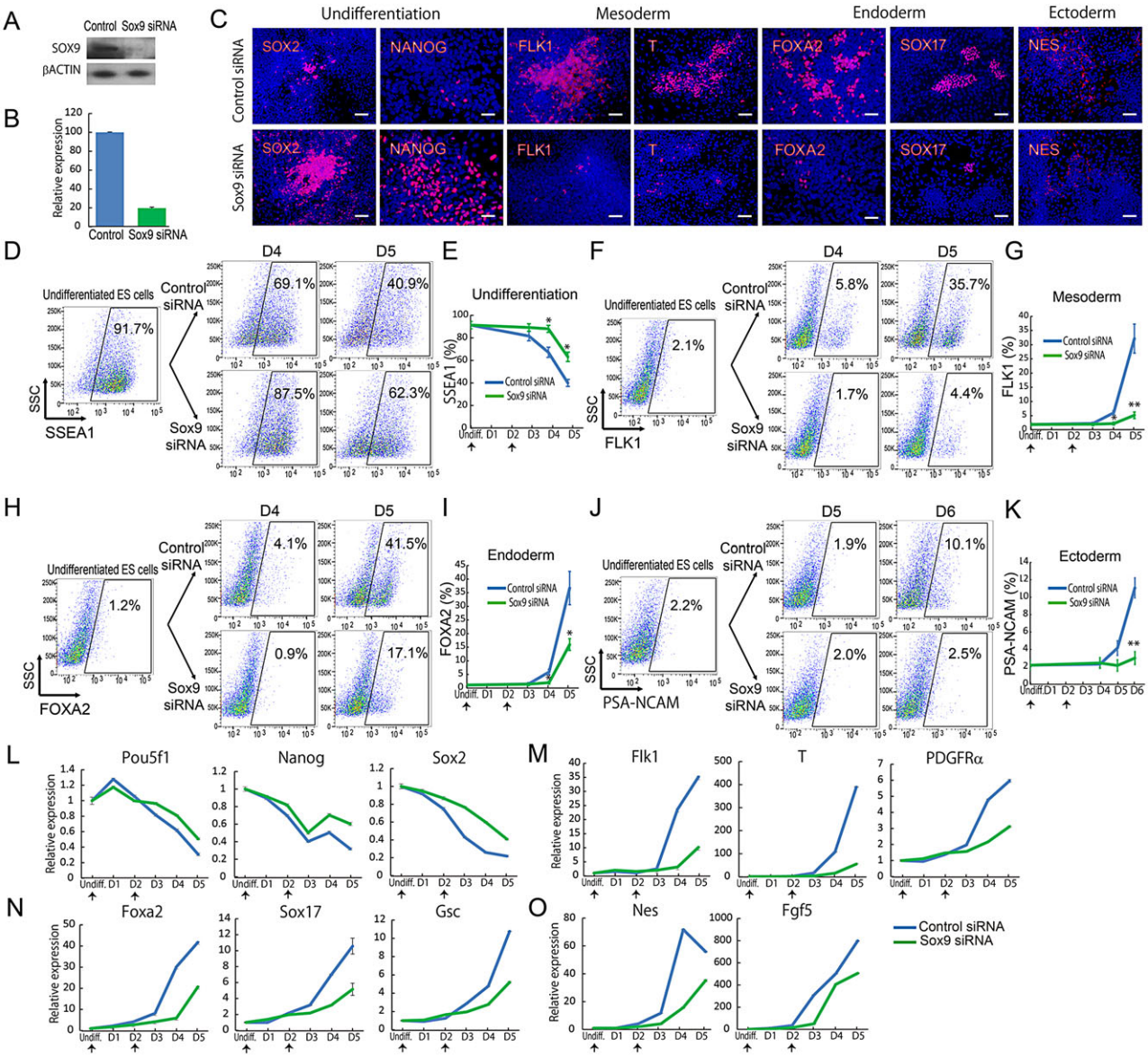

Fig. 5. Blocking the activation of endogenous *Sox9* represses the differentiation of ESCs. (A) Western blots detecting SOX9 and β-actin (control) in ESCs cultured for 5 days after treating with siRNAs against SOX9 or control siRNA. (B) qPCR analysis showing the mRNA levels of SOX9 in ESCs cultured for 5 days after treating with siRNAs against SOX9 or control siRNA. (C) Representative microscopic images of ESCs cultured for 5 days after treating with siRNAs against SOX9 or control and immunostained with pluripotency markers (SOX2, NANOG), mesoderm markers (FLK1, T), endoderm markers (FOXA2, SOX17) and ectoderm markers (NES). Scale bars: 200 μm. (D,F,H,J) Examples of FACS analyses: ESCs cultured for 4 days (D4), 5 days (D5) or 6 days (D6) after treating with siRNAs against SOX9 or control, and stained for $FLK1^+$, $FOXA2^+$ or $PSA\text{-}NCAM^+$. (E,G,I,K) A summary of three independent FACS experiments (data are mean±s.e.m.; $^*P<0.05$ and $^{**}P<0.01$ versus control siRNA). (L-O) qPCR analyses showing the expression changes ofpluripotent markers (*Pou5f1*, *Nanog*, *Sox2*) (L), mesoderm markers (*Flk1*, *T*, *Pdgfra*) (M), endoderm markers (*Foxa2*, *Sox17*, *Gsc*) (N) and ectoderm markers (*Nes*, *Fgf5*) (O) in ESCs after treating with siRNAs against SOX9 or control siRNA. Arrows show the timing (D0 and D2) of treatment.

expression of *Sox2* in pluripotent stem cells is located ∼4 kb downstream of the single *Sox2*-coding exon (Fig. 6F) (Tomioka et al., 2002; Sikorska et al., 2008; Miyagi et al., 2004). To test the possibility of a direct binding of P21 to the SRR2 enhancer, we performed chromatin immunoprecipitation (ChIP) assays with an anti-P21 antibody. As expected, we observed a specific binding of P21 to the SRR2 enhancer of *Sox2* on D5 under the control conditions (Dox+), whereas P21 did not bind to the UTR of *Sox2* or the *Nanog* promoter. Interestingly, the overexpression of *Sox9* (Dox−) significantly enhanced the direct binding of P21 to the SRR2 enhancer as early as D1 (Fig. 6G), which preceded the decrease of *Sox2* and the accelerated differentiation into three germ layers.

Effects of *Sox9* on early differentiation are dependent on *p21*

To investigate whether the regulation of accelerated differentiation by *Sox9* is mediated by P21, we blocked the expression of *p21* by treating cells with a siRNA against *p21*. Western blotting and qPCR analyses showed that treating cells with a siRNA against *p21* decreased the expression of *p21* by 80% by D4 (Fig. 7A,B). Significant increases of mesoderm markers (T and FLK1), endoderm markers (SOX17 and FOXA2) and ectoderm markers (NES and PSA-NCAM) by *Sox9* overexpression were almost completely abolished by the inhibition of *p21* (Fig. 7C-K). However, early disappearance of pluripotency gene expression (SOX2 and SSEA1) induced by *Sox9* overexpression was cancelled

Development (2014) 141, 4254-4266 doi:10.1242/dev.115436

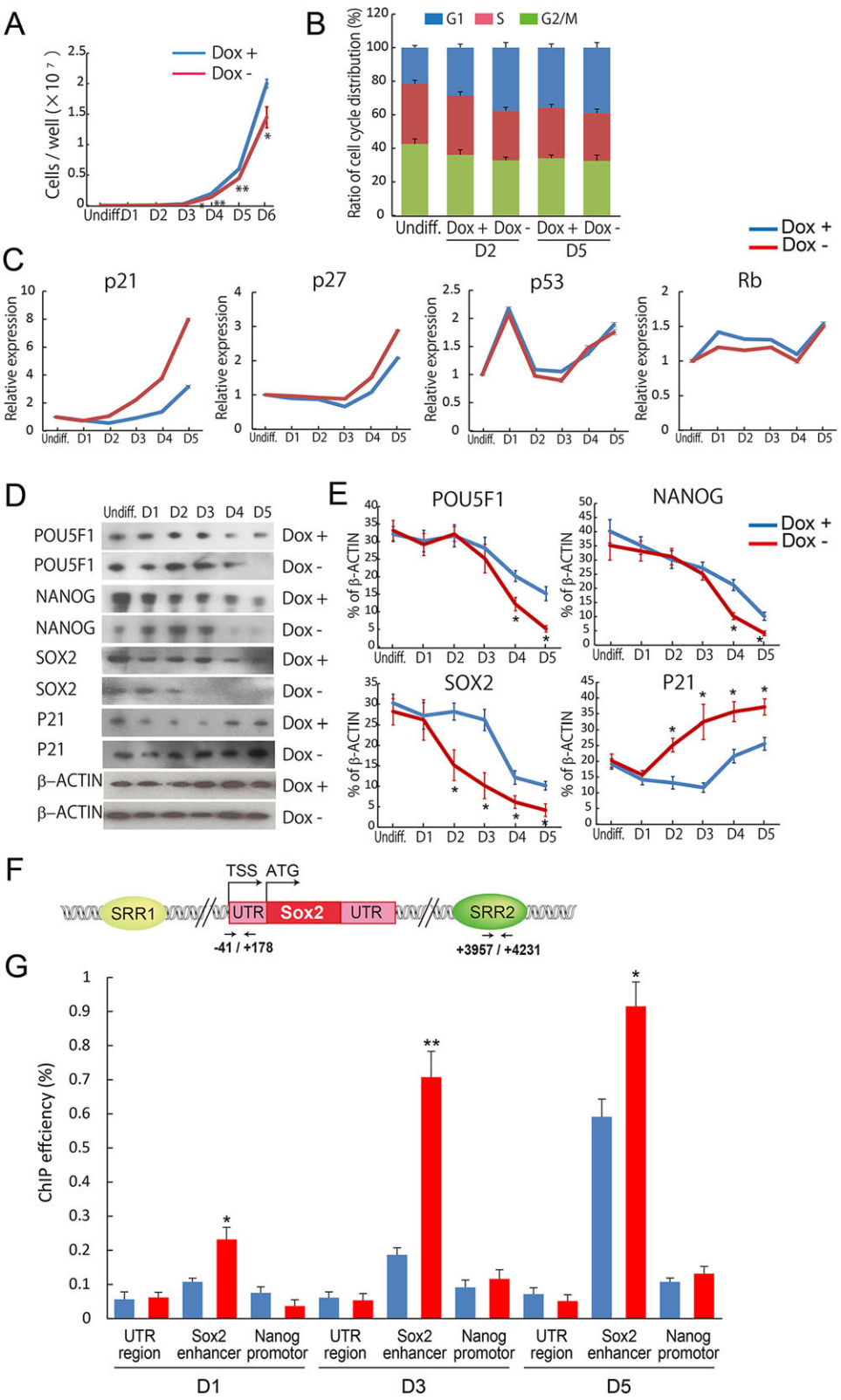

Fig. 6. *p21* (*Waf1*/*Cip1*) induced by *Sox9* inhibits *Sox2* expression through direct binding to SRR2 enhancer. (A) Growth profiles of SOX9-inducible ESCs cultured in Dox+ (control) or Dox– conditions (three independent experiments; data are mean±s.e.m.; **P*<0.05 and ***P*<0.01 versus Dox+). (B) Cell cycle profiles of SOX9-inducible ESCs cultured for 2 days (D2) or 5 days (D5) in Dox+ (control) or Dox– conditions (the independent experiments). (C) qPCR analyses showing the changes in expression of *p21*, *p27*, *p53* and *Rb* in SOX9-inducible ESCs cultured in Dox+ (control) or Dox– conditions. (D) Examples of western blots detecting POU5F1, NANOG, SOX2, P21 and β-actin (control) in SOX9-inducible ESCs cultured in Dox+ (control) or Dox– conditions. (E) A summary of three independent western blots, presented as a percent fraction of β-actin (data are mean±s.e.m.; **P*<0.05 versus Dox+). (F) Regulatory regions in the murine *Sox2* locus. (G) ChIP assays examining the binding of SOX9 to the UTR and the SRR2 enhancer region of *Sox2*, and to the *Nanog* promoter region in SOX9-inducible ESCs cultured after 1 day (D1), 3 days (D3) or 5 days (D5). Three independent experiments; data are mean±s.e.m.; **P*<0.05 and ***P*<0.01 versus Dox+. Red, Dox–; blue, Dox+.

by inhibiting *p21* (Fig. 7L-N). Furthermore, a ChIP assay revealed that direct binding of P21 in SRR2 enhancer of *Sox2* genes was completely abolished by treatment of siRNA against *p21*.

Next, we investigated whether the forced expression of *Sox2* on D2 can abolish the ESC differentiation induced by the overexpression of *Sox9*. Transfection of a plasmid vector expressing *Sox2* significantly abolished *Sox9*-elicited acceleration of the differentiation into the three germ layers from ESCs and also cancelled the early disappearance of the expression of pluripotency-related genes (supplementary material Fig. S5). These results indicate that the

Development (2014) 141, 4254-4266 doi:10.1242/dev.115436

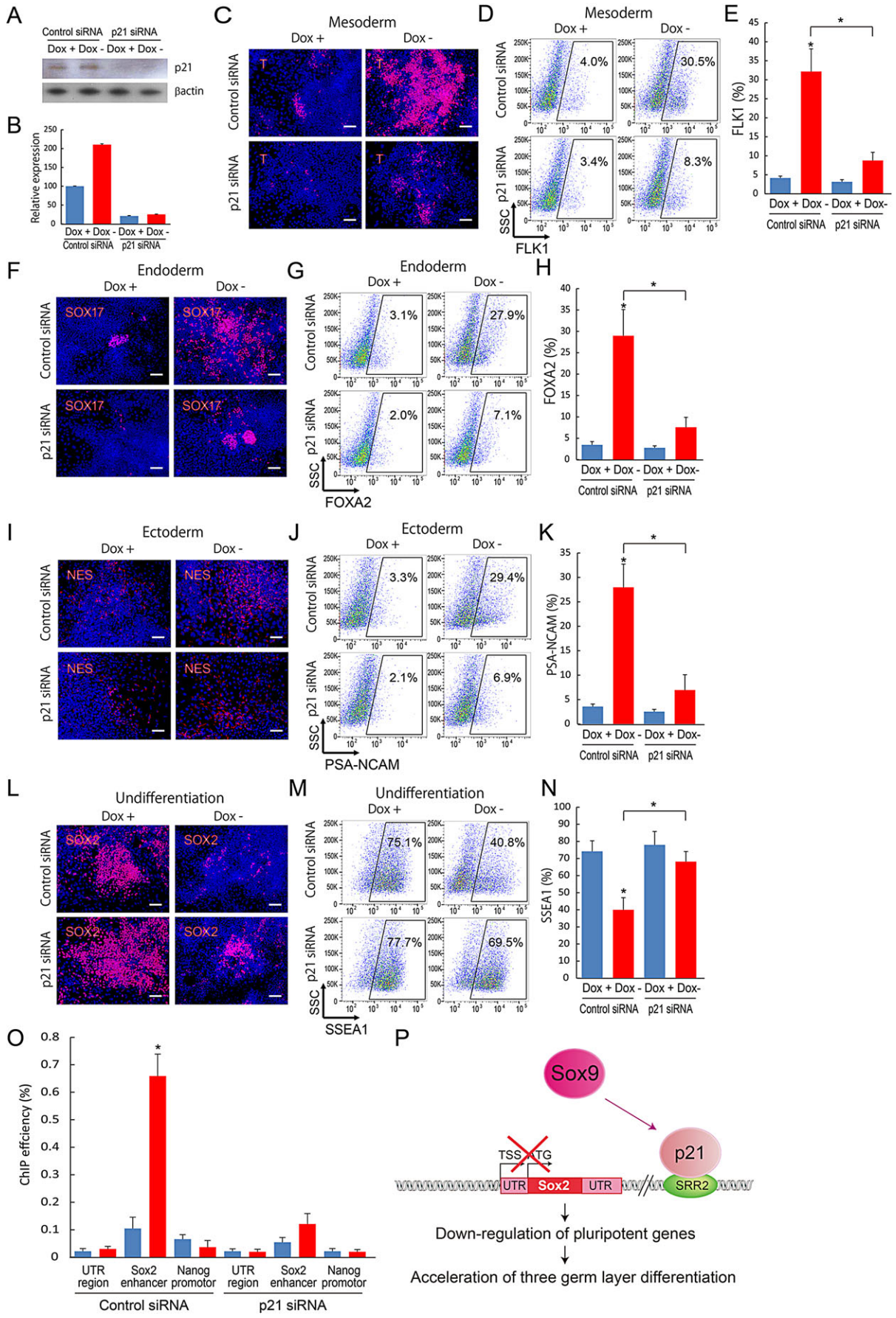

Fig. 7. See next page for legend.

Development (2014) 141, 4254-4266 doi:10.1242/dev.115436

Fig. 7. Effects of *Sox9* on early ESC differentiation requires *p21*. (A) Western blots detecting P21 and β-actin (control) in SOX9-inducible ESCs cultured for 4 days in Dox+ (control) or Dox– conditions after treating with siRNA against P21 or control siRNA. (B) qPCR analyses showing the expression of P21 and β-actin (control) in SOX9-inducible ESCs cultured in Dox+ (control) or Dox– conditions. (C,F,I,L) Immunostaining of SOX9-inducible ESCs cultured for 4 days in Dox+ (control) or Dox– conditions after treating with siRNAs against P21 or control siRNA: mesoderm marker (T), endoderm marker (SOX17), ectoderm marker (NES) and pluripotency marker (SOX2). Scale bars: 200 μm. (D,G,J,M) Examples of FACS analyses: SOX9-inducible ESCs cultured for 4 days (D,G,M) or 6 days (J) after treating with siRNA against P21 or control siRNA, and stained for $FLK1^+$, $FOXA2^+$ or $SSEA1^+$. (E,H,K,N) A summary of three independent FACS experiments (data are mean±s.e.m.; **P*<0.05 versus Dox+). (O) ChIP assays examining the binding of SOX9 to the UTR region and SRR2 enhancer region of SOX2, and to the *Nanog* promoter region in SOX9-inducible ESCs cultured for 3 days after treating with siRNAs against P21 or control siRNA (three independent experiments, data are mean±s.e.m.; **P*<0.05 versus Dox+). (P) A schematic diagram showing molecular interactions that regulate the differentiation of ESCs into three germ layers: *Sox9* induces *p21*, which then inhibits *Sox2* expression through its direct binding to the SRR2 enhancer of *Sox2* gene. Subsequently, other pluripotency genes, such as *Pou5f1* and *Nanog*, are downregulated, which accelerates the differentiation of ESCs into three germ layers.

overexpression of *Sox9* accelerates the differentiation into the three germ layers from ESCs through the *p21-Sox2* cascade (Fig. 7P).

Knockout of *Sox2* on D2 enhances the differentiation into the three germ layers

Finally, we examined whether the knockout of *Sox2* recapitulates phenotypes of *Sox9* overexpression using an inducible *Sox2*-null ESC line. Previous studies have shown that the knockout or knockdown of *Sox2* in ESCs differentiates ESCs into trophectoderm-like cells (Masui et al., 2007; Sharov et al., 2008; Nishiyama et al., 2013). Our results did not seem to be consistent with these well-established earlier findings, as the repression of SOX2 by the overexpression of SOX9 did not differentiate ESCs into trophoblast cells, but into three germ layers in our hands. Considering that the ability of early embryonic cells to give rise to the trophectoderm lineage is diminished at the epiblast stage of development, we hypothesized that the delay in *Sox2* knockout is responsible for the generation of three germ layers, but not trophectoderm-like cells. To test this notion, we compared two different protocols of *Sox2* knockout: for protocol 1 (Dox+, D0), Dox treatment is given from the start of differentiation (D0); for protocol 2 (Dox+, D2), Dox treatment is given from D2 (Fig. 8A-C). In protocol 1, the expression of *Sox2* diminished on D1, whereas in protocol 2 the expression of SOX2 diminished on D3 (Fig. 8A-C). The knockout of *Sox2* significantly decreased cell numbers during ESC differentiation (supplementary material Fig. S6A). FACS analysis also revealed that an increase in the cell population in G1 phase occurred in response to *Sox2* knockout from D2 (protocol 2; supplementary material Fig. S6B,C), showing similarity to *Sox9*-overexpressing effects during ESC differentiation. We then investigated the pluripotency state of these cells and their differentiation into trophectoderm cells or into three germ layers. Morphologically, many cells showed differentiation into trophectoderm-like cells with Dox treatment from D0 (Dox+, D0; protocol 1). These cells were positive for the expression of trophectoderm markers keratin 7 (KRT7) and cadherin 3 (CDH3). By contrast, the control condition (Dox−) and *Sox2* knockout from D2 (Dox+, D2; protocol 2) did not produce cells with trophectoderm-like morphology (Fig. 8D). Levels of pluripotency markers (SOX2 and NANOG) completely diminished by knockout of *Sox2* on D4 (Fig. 8E-G). Interestingly, SOX2 knockout from D0 (protocol 1) significantly increased SOX17- and FOXA2-positve endoderm cells, but suppressed the appearance of T- and FLK1-positive mesoderm cells and NES- and PSA-NCAM-positive ectoderm cells on D4 (Fig. 8E-G). *Sox2* knockout from D2 (protocol 2) significantly increased the numbers of T- and FLK1-positive mesoderm cells, SOX17- and FOXA2-positive endoderm cells, and NES- and PSA-NCAM-positive ectoderm cells on D4 (Fig. 8E-G). These results suggest that timing of *Sox2* knockout during cell differentiation is crucial for cell fate determination and that the delayed knockout of *Sox2* enhances the differentiation of ESCs into three germ layers (Fig. 8H).

DISCUSSION

Here, we have demonstrated a molecular mechanism involved in *Sox9*-mediated regulation of early differentiation of ESCs into three germ layers. *Sox9* stood out in unbiased analyses using 137 ESC clones of NIA mouse ESC bank. We showed the following functional links: *Sox9* increased *p21* expression; and P21 then inhibited Sox2 expression via direct binding in SRR enhancer. Although it has been shown that the repression of SOX2 in ESCs generates trophectoderm cells and endoderm cells (Masui et al., 2007; Nishiyama et al., 2009), the repression of SOX2 somewhat later during differentiation generates cells in all three germ layers (Fig. 8H), indicating that the timing of repression or activation of TFs is a crucial parameter in the determination of cell fate. This scenario may help to understand the initiation of stem cell differentiation and the finely controlled progenitor property.

In developmental biology, it is well established that TFs generally work in a cascade-like manner: early acting TFs initiate the differentiation, mid-acting TFs specify the cell lineage and late-acting TFs complete the process to finally form the maturely differentiated cells (Murry and Keller, 2008; Zaret and Grompe, 2008; Snykers et al., 2009). Although we and others have identified master and ancillary TFs for the determination of cell fate during the differentiation of ESCs (Vierbuchen et al., 2010; Ieda et al., 2010; Sekiya and Suzuki, 2011; Huang et al., 2011; Hiramatsu et al., 2011; Yamamizu et al., 2013), our approach using ESC lines with 137 TF transgenes successfully found the striking broad effects of SOX9 in promoting differentiation of ESCs into three germ layers by SOX9. Such a broad differentiation spectrum is most likely mediated by the SOX9-P21-SOX2 cascade, which seems to be a unique and distinct mechanism through which SOX9 acts. By contrast, the overexpression of other TFs (e.g. Cdx2) causes the differentiation into a rather specific lineage (e.g. trophectoderm), which is mediated by the direct activation of lineage-specific genes and the simultaneous repression of many downstream targets of pluripotency genes (e.g. *Pou5f1*, *Sox2* and *Nanog*) (Nishiyama et al., 2009). Obviously, it remains to be investigated whether the regulatory mechanisms found in ESCs also function during normal animal development.

Although SOX9 and SOX2 belong to the same Sox gene family, they seem to have distinct functions. SOX2, which is classified as a member of the SoxB1 family, interacts with other TFs that have POU domain proteins, including POU5F1 for pluripotency and POU3F2 for neural progenitors (Kondoh and Kamachi, 2010). The expression of most pluripotency-associated genes, including *Fgf4*, *Utf1*, *Foxo15*, *Lefty* and *Nanog*, is regulated by an enhancer containing SOX2- and POU5F1-binding motifs, which is highly active in undifferentiated ESCs but is no longer active in differentiated cells (Masui et al., 2007). In the neural stem cells of the developing embryo, co-expressing SOX2 and POU3F2 contributes to the maintenance of neural stem cell state by regulating NES expression (Tanaka et al., 2004; Miyagi et al., 2006). Thus, the combination of SOX2 with partner factors provides a code of cell specification. By

Development (2014) 141, 4254-4266 doi:10.1242/dev.115436

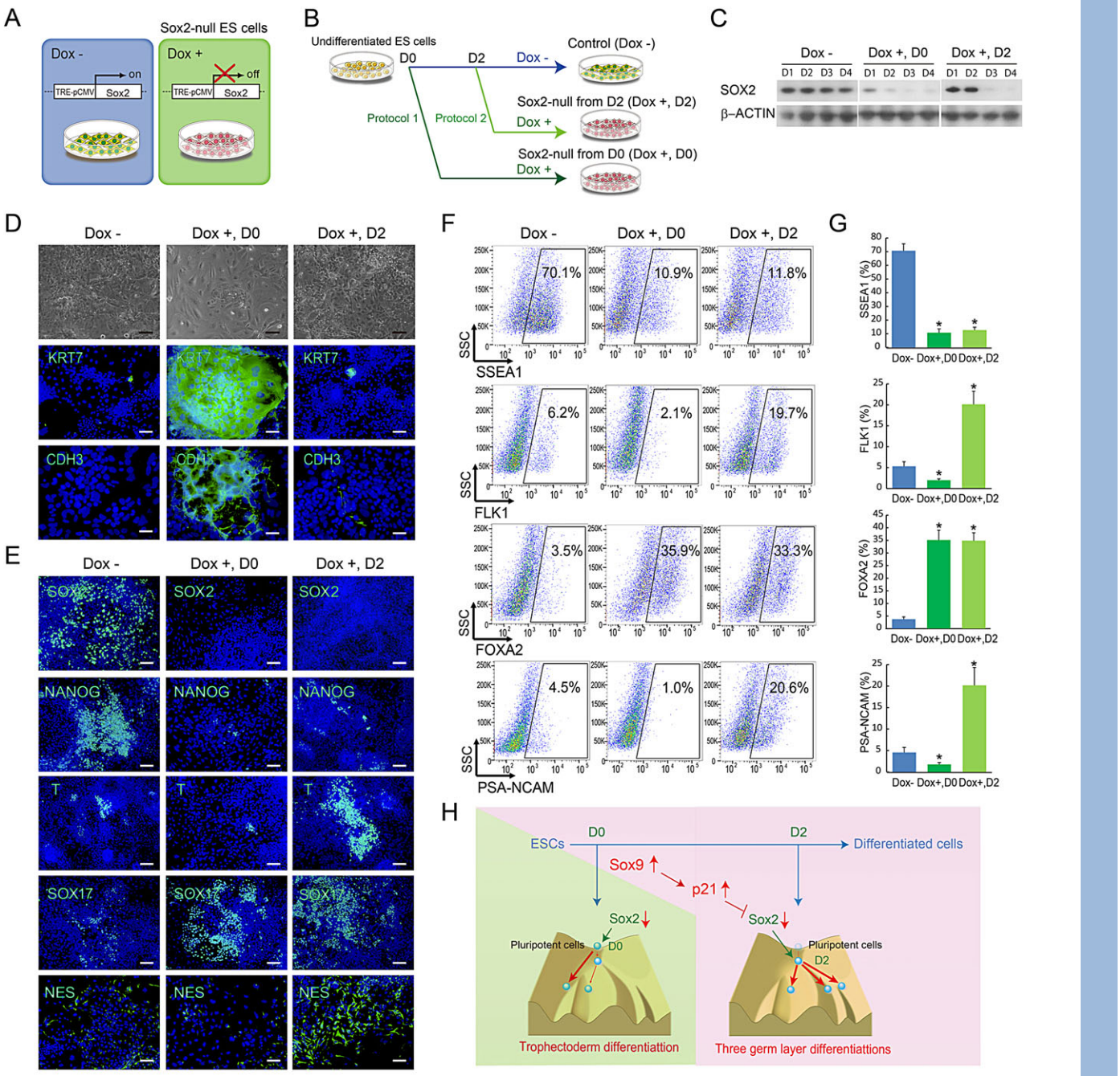

Fig. 8. Knockout of *Sox2* on day 2 enhances the differentiation into three germ layers. (A) Schematic diagram of inducible-SOX2 knockout ESCs (Masui et al., 2007). (B) Schematic diagram presenting two experimental protocols: in protocol 1 (Dox+, D0), Dox treatment begins at the start of differentiation (D0); in protocol 2 (Dox+, D2), Dox treatment begins on day 2 (D2). (C) Western blots detecting SOX2 and β-actin (control) in inducible-SOX2 knockout ESCs cultured in Dox– (control), protocol 1 or protocol 2 conditions. (D) Microscopic images of inducible-SOX2 knockout ESCs cultured for 4 days in Dox– (control), protocol 1 or protocol 2 conditions, and immunostained with trophectoderm markers (KRT7 or CDH3). (E) Microscopic images of inducible-SOX2 knockout ESCs cultured for 4 days in Dox– (control), protocol 1 or protocol 2 conditions, and immunostained for SOX2, NANOG, T, SOX17 and NES. Scale bar: 100 µm. (F) Examples of FACS analyses: inducible-SOX2 knockout ESCs cultured for 4 days (SSEA1, FLK1, FOXA2) or 6 days (PSA-NCAM) in Dox– (control), protocol 1 or protocol 2 conditions, and stained for SSEA1^{+}, FLK1^{+} or FOXA2^{+}. (G) Summary of three independent FACS experiments (data are mean±s.e.m.; *P<0.05 versus Dox+). (H) A model for cell fate determination governed by SOX2: the repression of SOX2 from D0 enhances the differentiation of ESCs into trophectoderm cells and endoderm cells, whereas the repression of SOX2 from D2 enhances the differentiation of ESCs into three germ layers, indicating that the timing of SOX2 repression is crucial for the cell fate determination.

contrast, SOX9, which is classified as a SoxE family member, has a dimerization domain and mainly functions in organ development as a dimer (Kondoh and Kamachi, 2010; Lefebvre et al., 2007). Although the SOX9 dimer directly binds to promote transcription of specific genes, in depth investigations of the molecular interactions and post-transcriptional regulation of SOX9 are needed to determine how it activates different groups of genes in different cell types. In this sense, several post-translational modifications of SOX9 can help to understand the level of its activity. Phosphorylation by protein kinase A (PKA) on two sites that flank the HMG box domain result

Development (2014) 141, 4254-4266 doi:10.1242/dev.115436

in an increase of SOX9-binding affinity to DNA (Huang et al., 2000). PKA signaling accelerates the onset of differentiation into three germ layers through expression of the H3K9 methyltransferase G9a (Yamamizu et al., 2012a). Furthermore, PKA turns on in the early blastocyte stages of development and regulates early differentiation of the mouse embryo (Yamamizu et al., 2012a). Furthermore, SOX9 can be sumoylated, with variable consequences for protein stability, nuclear localization, DNA-binding efficiency and transactivation potential (Taylor and Labonne, 2005; Hattori et al., 2006). PKA and sumoylation add to the network that regulates SOX9 function in various cell types.

The paradigm identified here in ESC differentiation may apply to other stem cells and progenitors, and also to cancer cells. SOX9 is highly expressed in cancers of the skin, prostate, lung, colon and brain (Kordes and Hagel, 2006; Vidal et al., 2008; Wang et al., 2008; Jiang et al., 2010; Matheu et al., 2012). However, whether SOX9 has an effect on tumor growth is still controversial. SOX9 has shown several pro-oncogenic properties, including the ability to promote proliferation, to inhibit senescence and to collaborate with other oncogenes in neoplastic transformation (Wang et al., 2008; Jiang et al., 2010; Matheu et al., 2012). But some reports demonstrated that overexpression of SOX9 in human melanoma or human endometrial carcinoma, as well as in chondrocytes, inhibited cell proliferation through P21 expression in cooperation with p53 (Panda et al., 2001; Passeron et al., 2009; Saegusa et al., 2012). Variable outcomes are likely to be correlated with the relative activation of P21. P21 regulates functions of many progenitors and stem cells, including cancer stem cells, neural stem cells (NSCs), hematopoietic stem cells (HSCs), hair follicle stem cells, mesenchymal stem cells and ESC/iPSCs (van den Bos et al., 1998; Kippin et al., 2005; Orford and Scadden, 2008; Moriguchi et al., 2010; Dolezalova et al., 2012; Lee et al., 2013). P21 governs self-renewal of colon cancer-initiating cells through cell-cycle restriction and protection from DNA damage accumulation (O'Brien et al., 2012). In NSCs and HSCs, cell cycle restriction by P21 appears to be crucial for self-renewal, as P21-deficient NSCs and HSCs proliferate more actively but are depleted over time (Kippin et al., 2005; Orford and Scadden, 2008).

Overall, SOX9 has two special features. First, its widespread positive transcription factor activity. It is noteworthy that, in spite of its extensive function, *Sox9* haploinsufficiency results in campomelic dysplasia, which is mainly characterized by skeletal malformation, XY sex reversal and neonatal lethality (Foster et al., 1994; Wagner et al., 1994; Bi et al., 2001; Chaboissier et al., 2004). This may indicate that one active allele is sufficient in cell types that have a lesser requirement for SOX9 activity. The large spectrum of action of SOX9 is logically related to its second feature: the general inhibitory action on SOX2 that we describe. Our work is consistent with a recent study showing that P21 control adult neural stem cell expansion by negatively regulating SOX2 induction by direct binding of SRR2 enhancer (Marqués-Torrejon et al., 2013). In the more extensive study here, the attendant release from the pluripotential state initiates differentiation of ESCs. To this end, SOX9 itself must be transcribed efficiently at an early phase in ESC differentiation and thereafter in many tissues. This transcription now becomes the target of further work.

MATERIALS AND METHODS

Cell culture and differentiation

Mouse ESC lines carrying a tetracycline-regulatable TF (Nishiyama et al., 2009; Correa-Cerro et al., 2011) and tetracycline-regulatable *Sox2*-null ESCs (Masui et al., 2007) were cultured and differentiated as described previously (Yamamizu et al., 2009, 2012a). The organ-specific cell culture media have also been described previously (Yamamizu et al., 2013). Differentiated cells were examined by immunostaining and flow cytometric analysis.

FACS analysis

Cultured cells were harvested in differentiation medium (DM) (Yamamizu et al., 2009, 2012a) or in DM and culture medium for neurons (Yamamizu et al., 2013) at 4, 5 and 6 days after differentiation, and stained with APC-conjugated anti-FLK1 antibody MoAb (eBioscience, 17-5821; 1:50), APC-conjugated anti-PSA-NCAM antibody MoAb (Miltenyi Biotec, 130-093-273; 1:50), PE-conjugated anti-SSEA1 antibody MoAb (R&D Systems, FAB2155P; 1:50) or APC-conjugated anti-CDH5 antibody MoAb (eBioscience, FAB761A; 1:50) and then subjected to analysis using FACS Canto II (Becton Dickinson) (Yamamizu et al., 2013). For intracellular proteins, cultured cells were fixed with 4% paraformaldehyde and washed by PBS with 5% FCS and 0.75% saponin (Sigma-Aldrich) (Yamamizu et al., 2012b, 2013). Fixed cells were stained with PE-conjugated anti-FOXA2 antibody (Bioss, bs-2358R-PE; 1:50) and then subjected to analysis using FACS Canto II (Becton Dickinson).

For cell cycle analysis, the differentiated cells were fixed in 70% ethanol and 100 µg/ml RNase (Sigma-Aldrich) was added for removal of RNA. The cells were stained with 5 µg/ml propidium iodide (Roche) at 4°C for 1 h and then subjected to analysis using FACS Canto II (Becton Dickinson).

Immunohistochemistry and alkaline phosphatase staining

Immunostaining for cultured cells was carried out as described previously (Yamamizu et al., 2009, 2012a). Primary antibodies were as follows: mouse anti-POU5F1 (Santa Cruz, 5279; 1:200); rabbit anti-NANOG (ReproCell, RCAB0002P; 1:500); rat anti-SOX2 (eBioscience; 1:500); mouse anti-SSEA1 (R&D Systems, FAB2155P; 1:500); rat anti-FLK1 (eBioscience, 14-5821; 1:500); goat anti-T (R&D Systems, AF2085; 1:500); rat anti-CD31 (eBioscience, 557355; 1:50); rat anti-CDH5 (eBioscience, MAB3226; 1:500); rabbit anti-FOXA2 (Millipore, 07-633; 1:500); goat anti-SOX17 (R&D Systems, AF1924; 1:500); mouse anti-ALB (R&D Systems, MAB1455; 1:200); mouse anti-NES (StemCell Technologies, 01418; 1:500); mouse anti-βIII-TUBULIN (TUJ1) (Covance, MMS-435P; 1:500); rabbit anti-TUJ1 (Covance, MRB-435P; 1:500); mouse anti-MAP2 (Sigma-Aldrich, M4403; 1:500); mouse anti-ISL1/ISL2 (DSHB, 81.5C10-c; 1:500); and rabbit anti-GABA (Sigma-Aldrich, A2052; 1:500).

For alkaline phosphatase staining, differentiated cells were stained using an alkaline phosphatase kit (Sigma-Aldrich) according to the manufacturer's instruction. Undifferentiated ESC colonies, partially differentiated cell colonies and totally differentiated cell colonies were evaluated by AP staining as follows: undifferentiated, AP-positive cells only; partially differentiated, mixture of AP-positive and -negative cells; totally differentiated, AP-negative cells only (Yamamizu et al., 2012a).

Western blotting

Western blot was performed as previously described (Yamamizu et al., 2010). Briefly, undifferentiated and differentiated cells were lysed in lysis buffer, and the samples were run on SDS/polyacrylamide gel electrophoresis, using a gradient gel (Invitrogen) followed by electrophoretic transfer onto nitrocellulose membranes with iBlot (Invitrogen). After the blots were incubated for 1 h in 5% skim milk, they were incubated overnight with the respective primary antibodies at 4°C. Primary antibodies were as follows: rabbit anti-SOX9 (Abcam, ab3697; 1:1000); mouse anti-FLAG (Sigma-Aldrich, F1804; 1:1000); mouse anti-POU5F1 (Santa Cruz, 5279; 1:1000); rabbit anti-NANOG (ReproCell, RCA0002P; 1:1000); rat anti-SOX2 (eBioscience, 14-9811-82; 1:1000); rabbit anti-P21 (Invitrogen, ab7960; 1:500); and mouse anti-β-actin (Sigma-Aldrich, A5441; 1:5000). Anti-mouse, anti-rabbit or anti-rat IgG antibodies conjugated with horseradish peroxidase (HRP) were used as secondary antibodies (1:10,000). Can Get Signal Immunoreaction Enhancer solution kit (Toyobo) was used for signal enhancement. Immunoreactivity was detected with the enhanced Pierce ECL Western Blotting Substrate (Thermo Scientific). Signal intensity was calculated with Scion Image software (Scion).

Development (2014) 141, 4254-4266 doi:10.1242/dev.115436

RNA isolation and quantitative reverse-transcription polymerase chain reaction

Total RNA was isolated from cells in undifferentiated ESCs and differentiated cells, using Trizol (Invitrogen), according to the manufacturer's instructions. Reverse transcription was performed with the SuperScript III first-strand synthesis system (Invitrogen). Quantitative PCR (qPCR) was performed using Power SYBR Green PCR Master Mix (Applied Biosystems) and an ABI7300 system (Applied Biosystems). The amount of target RNA was determined from the appropriate standard curve and normalized relative to the amount of *Gapdh* mRNA. Primer sequences are shown in supplementary material Table S1.

Microarray analysis

Microarray analyses were carried out as described previously (Nishiyama et al., 2009; Correa-Cerro et al., 2011).

PAS staining, LDL uptake and albumin ELISA assays

Cells on day 7 of differentiation were fixed by 4% paraformaldehyde and stained by periodic acid-Schiff (PAS, Sigma) according to the manufacturer's instruction. LDL uptake by cells was assessed by fluorescence microscopy after incubation of the differentiated cells with 10 µg/ml acetylated LDL labeled with 1,1′-dioctadecyl-3,3,3′,3′-tetramethylindo-carbocyanine perchlorate (DiI-Ac-LDL) (Biomedical Technologies) for 4 h at 37°C and DAPI. The amounts of mouse ALB secreted in the culture media [DMEM without glucose or Phenol Red (Invitrogen) supplemented with 2 mM sodium pyruvate (Sigma-Aldrich) and 20 mM sodium lactate (Sigma-Aldrich)] were measured after culture of differentiated cells from ESCs or adult mouse primary hepatocytes for 24 h using a Mouse Albumin ELISA Kit (Bethyl Laboratory) according to the manufacturer's instructions. The absorbance was measured with a VICTOR^3 V microplate reader (PerkinElmer).

SOX9 or P21 knockdown using siRNA

siRNA targeting mouse SOX9, P21 and negative control were purchased from Invitrogen (Stealth RNAi). Stealth RNAi for SOX9 or P21, or control siRNA (10 nM) were transfected at D0 and D2 using Lipofectamine RNAiMAX (Invitrogen) according to the manufacturer's instruction. Differentiated cells were examined by immunohistochemistry, FACS analysis and qPCR.

Chromatin immunoprecipitation

After 1, 3 or 5 days, differentiated cells were subjected to crosslinking with 1% formaldehyde. Chromatin was digested in the buffer containing 0.1% sodium deoxycholate and then sheared to DNA fragments with an average length of 100-500 bp. Sonicated DNA was subjected to immunoprecipitation using anti-P21 antibody (Invitrogen). Immunoprecipitated DNA was reverse-crosslinked and qPCR was performed using Power SYBR Green PCR Master Mix (Applied Biosystems). Sets of primers were used to amplify DNA sequences (supplementary material Table S2) (Marqués-Torrejon et al., 2013; Li et al., 2012). PCR amplification was conducted with a variable number of cycles (94°C for 30 s, 60°C for 30 s and 72°C for 30 s).

Statistical analysis

At least three independent experiments were performed. Statistical analysis of the data was performed with ANOVA. $P<0.05$ was considered significant. Values are reported as mean±s.e.m.

Accession number

The GEO accession number for microarray data reported in this paper is GSE31381.

Acknowledgements

We thank our lab members for the production and early analyses of the NIA mouse ESC bank. We also thank Dr Hitoshi Niwa for providing an inducible SOX2-null ESCs.

Competing interests

The authors declare no competing financial interests.

Author contributions

K.Y. performed all experiments and wrote the manuscript; D.S. supervised the project; M.S.H.K. supervised all experiments and wrote the manuscript.

Funding

This research was supported in part by the Intramural Research Program of the National Institutes of Health (NIH), National Institute on Aging. This research was also supported in part by the Japan Science and Technology Agency (JST), CREST program and Research Center Network for Realization of Regenerative Medicine program. K.Y. was supported by the postdoctoral fellowships from the Kanae Foundation (Japan), Uehara Memorial Foundation (Japan), Naito Foundation (Japan) and the Japan Society for Promotion of Science (JSPS). Deposited in PMC for release after 12 months.

Supplementary material

Supplementary material available online at
http://dev.biologists.org/lookup/suppl/doi:10.1242/dev.115436/-/DC1

References

Akiyama, H., Kim, J.-E., Nakashima, K., Balmes, G., Iwai, N., Deng, J. M., Zhang, Z., Martin, J. F., Behringer, R. R., Nakamura, T. et al. (2005). Osteo-chondroprogenitor cells are derived from Sox9 expressing precursors. *Proc. Natl. Acad. Sci. USA* **102**, 14665-14670.

Becker, K. A., Ghule, P. N., Therrien, J. A., Lian, J. B., Stein, J. L., van Wijnen, A. J. and Stein, G. S. (2006). Self-renewal of human embryonic stem cells is supported by a shortened G1 cell cycle phase. *J. Cell Physiol.* **209**, 883-893.

Besson, A., Dowdy, S. F. and Roberts, J. M. (2008). CDK inhibitors: cell cycle regulators and beyond. *Dev. Cell* **14**, 159-169.

Bi, W., Huang, W., Whitworth, D. J., Deng, J. M., Zhang, Z., Behringer, R. R. and de Crombrugghe, B. (2001). Haploinsufficiency of Sox9 results in defective cartilage primordia and premature skeletal mineralization. *Proc. Natl. Acad. Sci. USA* **98**, 6698-6703.

Chaboissier, M.-C., Kobayashi, A., Vidal, V. I. P., Lützkendorf, S., van de Kant, H. J. G., Wegner, M., de Rooij, D. G., Behringer, R. R. and Schedl, A. (2004). Functional analysis of Sox8 and Sox9 during sex determination in the mouse. *Development* **131**, 1891-1901.

Collins, F. S., Rossant, J. and Wurst, W. (2007). A mouse for all reasons. *Cell* **128**, 9-13.

Correa-Cerro, L. S., Piao, Y., Sharov, A. A., Nishiyama, A., Cadet, J. S., Yu, H., Sharova, L. V., Xin, L., Hoang, H. G., Thomas, M. et al. (2011). Generation of mouse ES cell lines engineered for the forced induction of transcription factors. *Sci. Rep.* **1**, 167.

Davis, R. L., Weintraub, H. and Lassar, A. B. (1987). Expression of a single transfected cDNA converts fibroblasts to myoblasts. *Cell* **51**, 987-1000.

Devgan, V., Mammucari, C., Millar, S. E., Brisken, C. and Dotto, G. P. (2005). p21WAF1/Cip1 is a negative transcriptional regulator of Wnt4 expression downstream of Notch1 activation. *Genes Dev.* **19**, 1485-1495.

Dolezalova, D., Mraz, M., Barta, T., Plevova, K., Vinarsky, V., Holubcova, Z., Jaros, J., Dvorak, P., Pospisilova, S. and Hampl, A. (2012). MicroRNAs regulate p21(Waf1/Cip1) protein expression and the DNA damage response in human embryonic stem cells. *Stem Cells* **30**, 1362-1372.

Egozi, D., Shapira, M., Paor, G., Ben-Izhak, O., Skorecki, K. and Hershko, D. D. (2007). Regulation of the cell cycle inhibitor p27 and its ubiquitin ligase Skp2 in differentiation of human embryonic stem cells. *FASEB J.* **21**, 2807-2817.

Foster, J. W., Dominguez-Steglich, M. A., Guioli, S., Kwok, C., Weller, P. A., Stevanović, M., Weissenbach, J., Mansour, S., Young, I. D., Goodfellow, P. N. et al. (1994). Campomelic dysplasia and autosomal sex reversal caused by mutations in an SRY-related gene. *Nature* **372**, 525-530.

Furuyama, K., Kawaguchi, Y., Akiyama, H., Horiguchi, M., Kodama, S., Kuhara, T., Hosokawa, S., Elbahrawy, A., Soeda, T., Koizumi, M. et al. (2011). Continuous cell supply from a Sox9-expressing progenitor zone in adult liver, exocrine pancreas and intestine. *Nat. Genet.* **43**, 34-41.

Hattori, T., Eberspaecher, H., Lu, J., Zhang, R., Nishida, T., Kahyo, T., Yasuda, H. and de Crombrugghe, B. (2006). Interactions between PIAS proteins and SOX9 result in an increase in the cellular concentrations of SOX9. *J. Biol. Chem.* **281**, 14417-14428.

Hiramatsu, K., Sasagawa, S., Outani, H., Nakagawa, K., Yoshikawa, H. and Tsumaki, N. (2011). Generation of hyaline cartilaginous tissue from mouse adult dermal fibroblast culture by defined factors. *J. Clin. Invest.* **121**, 640-657.

Huang, W., Zhou, X., Lefebvre, V. and de Crombrugghe, B. (2000). Phosphorylation of SOX9 by cyclic AMP-dependent protein kinase A enhances SOX9's ability to transactivate a Col2a1 chondrocyte-specific enhancer. *Mol. Cell. Biol.* **20**, 4149-4158.

Huang, P., He, Z., Ji, S., Sun, H., Xiang, D., Liu, C., Hu, Y., Wang, X. and Hui, L. (2011). Induction of functional hepatocyte-like cells from mouse fibroblasts by defined factors. *Nature* **475**, 386-389.

Ieda, M., Fu, J.-D., Delgado-Olguin, P., Vedantham, V., Hayashi, Y., Bruneau, B. G. and Srivastava, D. (2010). Direct reprogramming of fibroblasts into functional cardiomyocytes by defined factors. *Cell* **142**, 375-386.

Ivanova, N., Dobrin, R., Lu, R., Kotenko, I., Levorse, J., DeCoste, C., Schafer, X., Lun, Y. and Lemischka, I. R. (2006). Dissecting self-renewal in stem cells with RNA interference. *Nature* **442**, 533-538.

Jiang, S. S., Fang, W.-T., Hou, Y.-H., Huang, S.-F., Yen, B. L., Chang, J.-L., Li, S.-M., Liu, H.-P., Liu, Y.-L., Huang, C.-T. et al. (2010). Upregulation of SOX9 in lung adenocarcinoma and its involvement in the regulation of cell growth and tumorigenicity. *Clin. Cancer Res.* **16**, 4363-4373.
Kadaja, M., Keyes, B. E., Lin, M., Pasolli, H. A., Genander, M., Polak, L., Stokes, N., Zheng, D. and Fuchs, E. (2014). SOX9: a stem cell transcriptional regulator of secreted niche signaling factors. *Genes Dev.* **28**, 328-341.
Kanamori, M., Konno, H., Osato, N., Kawai, J., Hayashizaki, Y. and Suzuki, H. (2004). A genome-wide and nonredundant mouse transcription factor database. *Biochem. Biophys. Res. Commun.* **322**, 787-793.
Kippin, T. E., Martens, D. J. and van der Kooy, D. (2005). p21 loss compromises the relative quiescence of forebrain stem cell proliferation leading to exhaustion of their proliferation capacity. *Genes Dev.* **19**, 756-767.
Kondoh, H. and Kamachi, Y. (2010). SOX-partner code for cell specification: regulatory target selection and underlying molecular mechanisms. *Int. J. Biochem. Cell Biol.* **42**, 391-399.
Kordes, U. and Hagel, C. (2006). Expression of SOX9 and SOX10 in central neuroepithelial tumor. *J. Neurooncol.* **80**, 151-155.
Lee, J., Hoi, C. S. L., Lilja, K. C., White, B. S., Lee, S. E., Shalloway, D. and Tumbar, T. (2013). Runx1 and p21 synergistically limit the extent of hair follicle stem cell quiescence in vivo. *Proc. Natl. Acad. Sci. USA* **110**, 4634-4639.
Lefebvre, V., Dumitriu, B., Penzo-Méndez, A., Han, Y. and Pallavi, B. (2007). Control of cell fate and differentiation by Sry-related high-mobility-group box (Sox) transcription factors. *Int. J. Biochem. Cell Biol.* **39**, 2195-2214.
Li, H., Collado, M., Villasante, A., Matheu, A., Lynch, C. J., Cañamero, M., Rizzoti, K., Carneiro, C., Martínez, G., Vidal, A. et al. (2012). p27(Kip1) directly represses Sox2 during embryonic stem cell differentiation. *Cell Stem Cell* **11**, 845-852.
Marqués-Torrejón, M. A., Porlan, E., Banito, A., Gómez-Ibarlucea, E., Lopez-Contreras, A. J., Fernández Capetillo, O., Vidal, A., Gil, J., Torres, J. and Fariñas, I. (2013). Cyclin-dependent kinase inhibitor p21 controls adult neural stem cell expansion by regulating Sox2 gene expression. *Cell Stem Cell* **12**, 88-100.
Masui, S., Nakatake, Y., Toyooka, Y., Shimosato, D., Yagi, R., Takahashi, K., Okochi, H., Okuda, A., Matoba, R., Sharov, A. A. et al. (2007). Pluripotency governed by Sox2 via regulation of Oct3/4 expression in mouse embryonic stem cells. *Nat. Cell Biol.* **9**, 625-635.
Matheu, A., Collado, M., Wise, C., Manterola, L., Cekaite, L., Tye, A. J., Canamero, M., Bujanda, L., Schedl, A., Cheah, K. S. E. et al. (2012). Oncogenicity of the developmental transcription factor Sox9. *Cancer Res.* **72**, 1301-1315.
Miyagi, S., Saito, T., Mizutani, K.-i., Masuyama, N., Gotoh, Y., Iwama, A., Nakauchi, H., Masui, S., Niwa, H., Nishimoto, M. et al. (2004). The Sox-2 regulatory regions display their activities in two distinct types of multipotent stem cells. *Mol. Cell. Biol.* **24**, 4207-4220.
Miyagi, S., Nishimoto, M., Saito, T., Ninomiya, M., Sawamoto, K., Okano, H., Muramatsu, M., Oguro, H., Iwama, A. and Okuda, A. (2006). The Sox2 regulatory region 2 functions as a neural stem cell-specific enhancer in the telencephalon. *J. Biol. Chem.* **281**, 13374-13381.
Moriguchi, H., Chung, R. T. and Sato, C. (2010). Tumorigenicity of human induced pluripotent stem cells depends on the balance of gene expression between p21 and p53. *Hepatology* **51**, 1088-1089.
Murry, C. E. and Keller, G. (2008). Differentiation of embryonic stem cells to clinically relevant populations: lessons from embryonic development. *Cell* **132**, 661-680.
Nishiyama, A., Xin, L., Sharov, A. A., Thomas, M., Mowrer, G., Meyers, E., Piao, Y., Mehta, S., Yee, S., Nakatake, Y. et al. (2009). Uncovering early response of gene regulatory networks in ESCs by systematic induction of transcription factors. *Cell Stem Cell* **5**, 420-433.
Nishiyama, A., Sharov, A. A., Piao, Y., Amano, M., Amano, T., Hoang, H. G., Binder, B. Y., Tapnio, R., Bassey, U., Malinou, J. N. et al. (2013). Systematic repression of transcription factors reveals limited patterns of gene expression changes in ES cells. *Sci. Rep.* **3**, 1390.
Orford, K. W. and Scadden, D. T. (2008). Deconstructing stem cell self-renewal: genetic insights into cell-cycle regulation. *Nat. Rev. Genet.* **9**, 115-128.
O'Brien, C. A., Kreso, A., Ryan, P., Hermans, K. G., Gibson, L., Wang, Y., Tsatsanis, A., Gallinger, S. and Dick, J. E. (2012). ID1 and ID3 regulate the self-renewal capacity of human colon cancer-initiating cells through p21. *Cancer Cell* **21**, 777-792.
Panda, D. K., Miao, D., Lefebvre, V., Hendy, G. N. and Goltzman, D. (2001). The transcription factor SOX9 regulates cell cycle and differentiation genes in chondrocytic CFK2 cells. *J. Biol. Chem.* **276**, 41229-41236.
Passeron, T., Valencia, J. C., Namiki, T., Vieira, W. D., Passeron, H., Miyamura, Y. and Hearing, V. J. (2009). Upregulation of SOX9 inhibits the growth of human and mouse melanomas and restores their sensitivity to retinoic acid. *J. Clin. Invest.* **119**, 954-963.
Saegusa, M., Hashimura, M., Suzuki, E., Yoshida, T. and Kuwata, T. (2012). Transcriptional up-regulation of Sox9 by NF-kappaB in endometrial carcinoma cells, modulating cell proliferation through alteration in the p14(ARF)/p53/p21 (WAF1) pathway. *Am. J. Pathol.* **181**, 684-692.
Sekiya, S. and Suzuki, A. (2011). Direct conversion of mouse fibroblasts to hepatocyte-like cells by defined factors. *Nature* **475**, 390-393.
Seymour, P. A., Freude, K. K., Tran, M. N., Mayes, E. E., Jensen, J., Kist, R., Scherer, G. and Sander, M. (2007). SOX9 is required for maintenance of the pancreatic progenitor cell pool. *Proc. Natl. Acad. Sci. USA* **104**, 1865-1870.
Sharov, A. A., Masui, S., Sharova, L. V., Piao, Y., Aiba, K., Matoba, R., Xin, L., Niwa, H. and Ko, M. S. H. (2008). Identification of Pou5f1, Sox2, and Nanog downstream target genes with statistical confidence by applying a novel algorithm to time course microarray and genome-wide chromatin immunoprecipitation data. *BMC Genomics* **9**, 269.
Sikorska, M., Sandhu, J. K., Deb-Rinker, P., Jezierski, A., LeBlanc, J., Charlebois, C., Ribecco-Lutkiewicz, M., Bani-Yaghoub, M. and Walker, P. R. (2008). Epigenetic modifications of SOX2 enhancers, SRR1 and SRR2, correlate with in vitro neural differentiation. *J. Neurosci. Res.* **86**, 1680-1693.
Skarnes, W. C., von Melchner, H., Wurst, W., Hicks, G., Nord, A. S., Cox, T., Young, S. G., Ruiz, P., Soriano, P., Tessier Lavigne, M. et al. (2004). A public gene trap resource for mouse functional genomics. *Nat. Genet.* **36**, 543-544.
Snykers, S., De Kock, J., Rogiers, V. and Vanhaecke, T. (2009). In vitro differentiation of embryonic and adult stem cells into hepatocytes: state of the art. *Stem Cells* **27**, 577-605.
Stolt, C. C., Lommes, P., Sock, E., Chaboissier, M.-C., Schedl, A. and Wegner, M. (2003). The Sox9 transcription factor determines glial fate choice in the developing spinal cord. *Genes Dev.* **17**, 1677-1689.
Su, A. I., Cooke, M. P., Ching, K. A., Hakak, Y., Walker, J. R., Wiltshire, T., Orth, A. P., Vega, R. G., Sapinoso, L. M., Moqrich, A. et al. (2002). Large-scale analysis of the human and mouse transcriptomes. *Proc. Natl. Acad. Sci. USA* **99**, 4465-4470.
Takahashi, K. and Yamanaka, S. (2006). Induction of pluripotent stem cells from mouse embryonic and adult fibroblast cultures by defined factors. *Cell* **126**, 663-676.
Tanaka, S., Kamachi, Y., Tanouchi, A., Hamada, H., Jing, N. and Kondoh, H. (2004). Interplay of SOX and POU factors in regulation of the Nestin gene in neural primordial cells. *Mol. Cell. Biol.* **24**, 8834-8846.
Taylor, K. M. and LaBonne, C. (2005). SoxE factors function equivalently during neural crest and inner ear development and their activity is regulated by SUMOylation. *Dev. Cell* **9**, 593-603.
Tomioka, M., Nishimoto, M., Miyagi, S., Katayanagi, T., Fukui, N., Niwa, H., Muramatsu, M. and Okuda, A. (2002). Identification of Sox-2 regulatory region which is under the control of Oct-3/4-Sox-2 complex. *Nucleic Acids Res.* **30**, 3202-3213.
van den Bos, C., Silverstetter, S., Murphy, M. and Connolly, T. (1998). p21(cip1) rescues human mesenchymal stem cells from apoptosis induced by low-density culture. *Cell Tissue Res.* **293**, 463-470.
Vidal, V. P. I., Chaboissier, M.-C., Lützkendorf, S., Cotsarelis, G., Mill, P., Hui, C.-C., Ortonne, N., Ortonne, J.-P. and Schedl, A. (2005). Sox9 is essential for outer root sheath differentiation and the formation of the hair stem cell compartment. *Curr. Biol.* **15**, 1340-1351.
Vidal, V. P. I., Ortonne, N. and Schedl, A. (2008). SOX9 expression is a general marker of basal cell carcinoma and adnexal-related neoplasms. *J. Cutan. Pathol.* **35**, 373-379.
Vierbuchen, T., Ostermeier, A., Pang, Z. P., Kokubu, Y., Südhof, T. C. and Wernig, M. (2010). Direct conversion of fibroblasts to functional neurons by defined factors. *Nature* **463**, 1035-1041.
Wagner, T., Wirth, J., Meyer, J., Zabel, B., Held, M., Zimmer, J., Pasantes, J., Bricarelli, F. D., Keutel, J., Hustert, E. et al. (1994). Autosomal sex reversal and campomelic dysplasia are caused by mutations in and around the SRY-related gene SOX9. *Cell* **79**, 1111-1120.
Wang, H., Leav, I., Ibaragi, S., Wegner, M., Hu, G.-F., Lu, M. L., Balk, S. P. and Yuan, X. (2008). SOX9 is expressed in human fetal prostate epithelium and enhances prostate cancer invasion. *Cancer Res.* **68**, 1625-1630.
Wu, C., Orozco, C., Boyer, J., Leglise, M., Goodale, J., Batalov, S., Hodge, C. L., Haase, J., Janes, J., Huss, J. W. III et al. (2009). BioGPS: an extensible and customizable portal for querying and organizing gene annotation resources. *Genome Biol.* **10**, R130.
Yamamizu, K., Kawasaki, K., Katayama, S., Watabe, T. and Yamashita, J. K. (2009). Enhancement of vascular progenitor potential by protein kinase A through dual induction of Flk-1 and Neuropilin-1. *Blood* **114**, 3707-3716.
Yamamizu, K., Matsunaga, T., Uosaki, H., Fukushima, H., Katayama, S., Hiraoka-Kanie, M., Mitani, K. and Yamashita, J. K. (2010). Convergence of Notch and beta-catenin signaling induces arterial fate in vascular progenitors. *J. Cell Biol.* **189**, 325-338.
Yamamizu, K., Fujihara, M., Tachibana, M., Katayama, S., Takahashi, A., Hara, E., Imai, H., Shinkai, Y. and Yamashita, J. K. (2012a). Protein kinase A determines timing of early differentiation through epigenetic regulation with G9a. *Cell Stem Cell* **10**, 759-770.
Yamamizu, K., Matsunaga, T., Katayama, S., Kataoka, H., Takayama, N., Eto, K., Nishikawa, S.-I. and Yamashita, J. K. (2012b). PKA/CREB signaling triggers initiation of endothelial and hematopoietic cell differentiation via Etv2 induction. *Stem Cells* **30**, 687-696.
Yamamizu, K., Piao, Y., Sharov, A. A., Zsiros, V., Yu, H., Nakazawa, K., Schlessinger, D. and Ko, M. S. H. (2013). Identification of transcription factors for lineage-specific ESC differentiation. *Stem Cell Reports* **1**, 545-559.
Zaret, K. S. and Grompe, M. (2008). Generation and regeneration of cells of the liver and pancreas. *Science* **322**, 1490-1494.

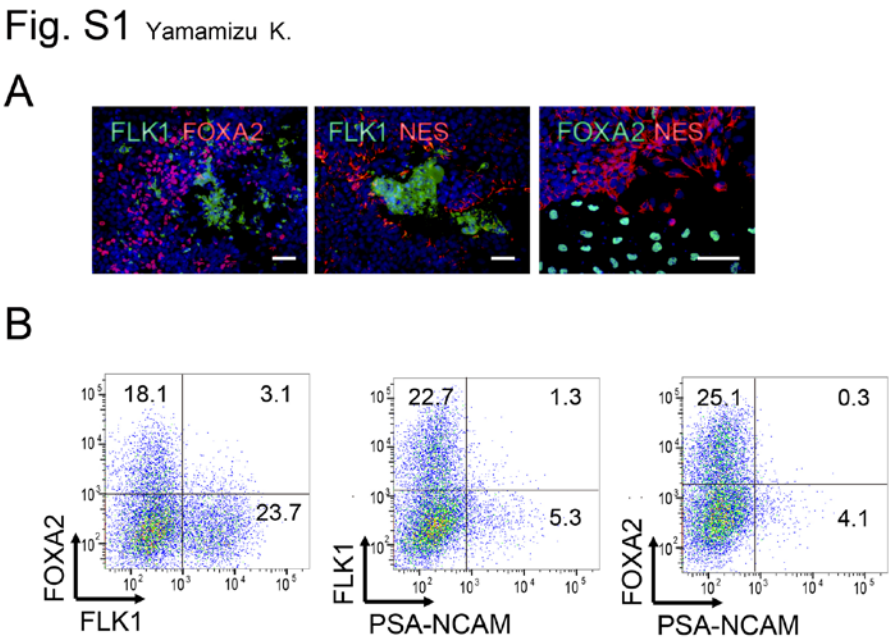

Fig. S1. Markers of different germ layers did not colocalize in the same cells. (A) Microscopic images of ESCs cultured for 5 days in the differentiation condition and stained with the combination of markers: FLK1 (mesoderm), FOXA2 (endoderm), or NES (ectoderm). Scale bar: 200 µm. (B) Examples of FACS analyses: ESCs cultured for 5 days in the differentiation condition and stained for the combination of markers: $FLK1^+$ and $FOXA2^+$, $FLK1^+$ and $PSA\text{-}NCAM^+$, or $FOXA2^+$ and $PSA\text{-}NCAM^+$.

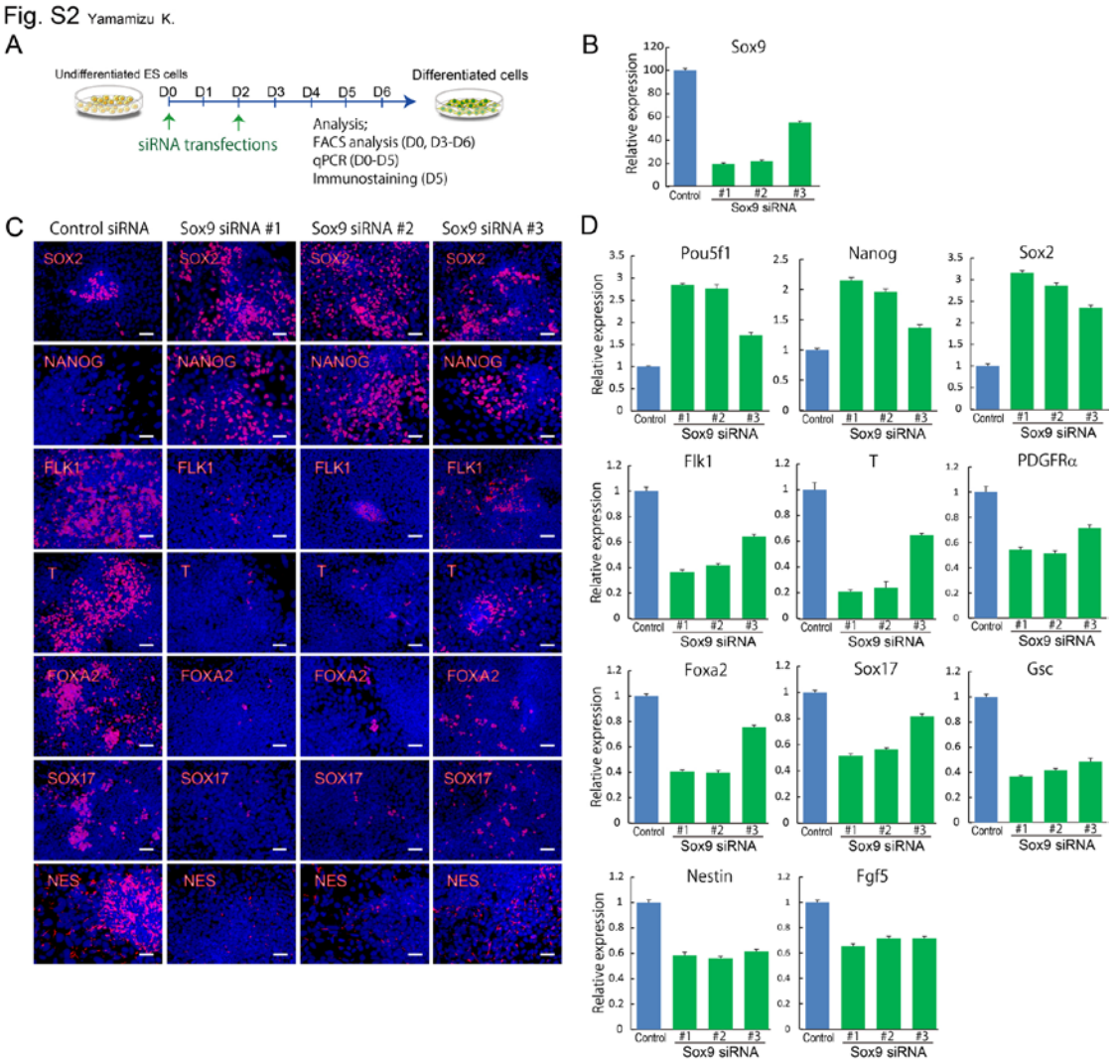

Fig. S2. Blocking the activation of endogenous *Sox9* inhibits the differentiation of ESCs into three germ layers. (A) Schematic diagram showing an experimental design. (B) qPCR analysis showing the mRNA expression of *Sox9* after treating cells with three independent siRNAs against *Sox9* or control. (C) Microscopy images of ESCs cultured for 5 days after treating with three independent siRNAs against Sox9 or control and stained with pluripotency markers (SOX2, NANOG), mesoderm markers (FLK1, T), endoderm markers (FOXA2, SOX17) and an ectoderm marker (NES). Scale bar: 200 µm. (D) qPCR analyses showing the mRNA expression of pluripotency markers (*Pou5f1*, *Nanog*, *Sox2*), mesoderm markers (*Flk1*, *T*, *PDGFRα*), endoderm markers (*Foxa2*, *Sox17*, *Gsc*) and ectoderm markers (*Nestin*, *Fgf5*) in ESCs cultured for 5 days after treating three independent siRNAs against Sox9 or control.

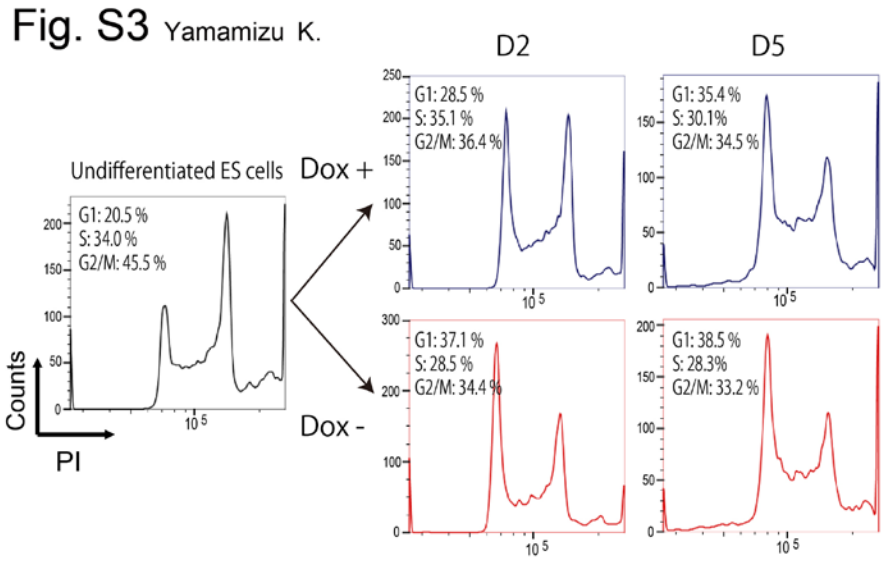

Fig. S3. Cell cycle profiles of Sox9-inducible ESCs by FACS analysis. FACS analysis showing cell cycle profiles of Sox9-inducible ESCs cultured for 2 days (D2) or 5 days (D5) in the Dox+ (control) or Dox– condition.

Fig. S4 Yamamizu K.

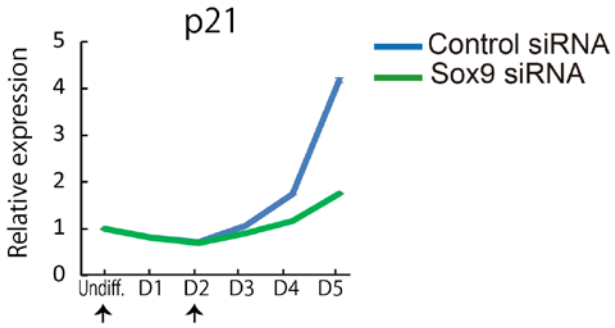

Fig. S4. Blocking the activation of endogenous Sox9 with an siRNA against Sox9 inhibits the increase of p21 expression that normally occurs from D4. qPCR analyses showing the expression changes of p21. Arrows show the timing (D0 and D2) of treatment of siRNA against Sox9 or control.

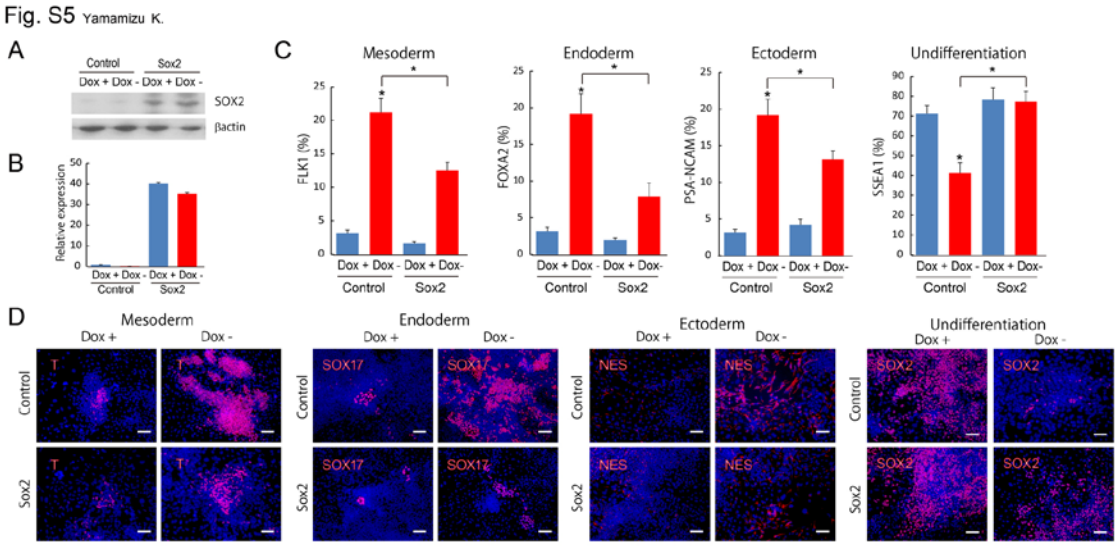

Fig. S5. Overexpression of *Sox2* prevents ESCs from differentiating into three germ layers, even when the exogenous *Sox9* was overexpressed. (A) Western blots detecting SOX2 and β-actin in Sox9-inducdible ESCs cultured for 4 days in the Dox+ (control) or Dox– condition. (B) A qPCR analysis showing the mRNA expression of *Sox2* in Sox9-inducible ESCs cultured for 4 days in the Dox+ (control) or Dox– condition after transfecting with a Sox2-expressing vector or a control vector. (C) Summary of FACS analyses: Sox9-inducible ESCs cultured for 4 days ($FLK1^+$, $FOXA2^+$ or $SSEA1^+$) or 6 days ($PSA\text{-}NCAM^+$) after transfecting with a Sox2-expressing vector or a control vector and stained for $FLK1^+$, $FOXA2^+$, $SSEA1^+$, or $PSA\text{-}NCAM^+$. (D) Microscopic images of Sox9-inducible ESCs cultured for 4 days after transfecting with a Sox2-expressing vector or a control vector and immunostained for T (mesoderm), SOX17 (endoderm), NES (ectoderm) and SOX2 (undifferentiation). Scale bar: 200 μm.

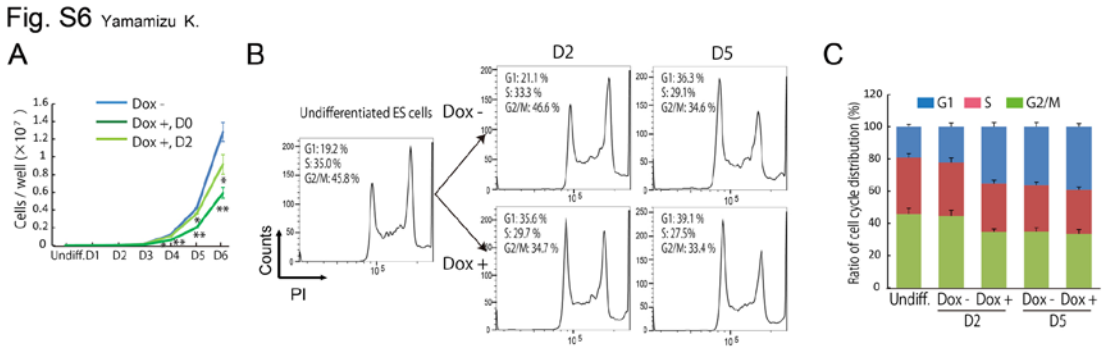

Fig. S6. Cell cycle profile of Sox2-repressible ESCs by FACS analysis. (A) Growth profiles of Sox2-repressible ESCs cultured in the Dox– (control), protocol 1 (Sox2-repressed from D0), or protocol 2 (Sox2-repressed from D2) (three independent experiments, SEM; **P*<0.05, ***P*<0.01 versus Dox+). (B,C) Cell cycle profiles of Sox2-repressible ESCs cultured for 2 days (D2) or 5 days (D5) in the Dox– (control) or Dox+ condition and analyzed by FACS (three independent experiments).

Supplementary material Table S1: Primer list for qPCR (related to Figs 2, 4-6)

Oct3/4 F	GGA CAT GAA AGC CCT GCA GAA
Oct3/4 R	GAC AGA TGG TGG TCT GGC TGA A
Nanog F	GAA TTC TGG GAA CGC CTC ATC
Nanog R	CCT TGT CAG CCT CAG GAC TTG
Sox2 F	AAC CGA TGC ACC GCT ACG A
Sox2 R	TGC TGC GAG TAG GAC ATG CTG
T F	GAA CAG CTC TCC AAC CTA TG
T R	AGA CTG GGA TAC TGG CTA GAG
Flk1 F	GGG ATG GTC CTT GCA TCA GAA
Flk1 R	ACT GGT AGC CAC TGG TCT GGT TG
PDGFRa F	CTT TGT GCC TCT CGG GAT GA
PDGFRa R	AGG TTA CTT GAG TCT CCG GAT CTG
Foxa2 F	GTC GTC CGA GCA GCA ACA TC
Foxa2 R	GGG TAG TGC ATG ACC TGT TCG TAG
Sox17 F	GGA CAC GAC TGC GGA GTG AA
Sox17 R	GGT CGG CAA CCG TCA AAT G
Gsc F	CCC GGT TCT GTA CTG GTG TC
Gsc R	AGC TGC TCA TCG GTG AAG AT
Nestin F	GGG CCA GCA CTC TTA GCT TTG ATA
Nestin R	TGA GCC TTC AGG GTG ATC CAG
Fgf5 F	AGT GTG CAG CGT CCA CAG AGA
Fgf5 R	TCC TAG TGT ATG CTT GGT GGA CAG A
Sox9 F	CTG AAG GGC TAC GAC TGG AC
Sox9 R	TAC TGG TCT GCC AGC TTC CT
p21 F	TTG CAC TCT GGT GTC TGA GC
p21 R	TCT GCG CTT GGA GTG ATA GA
p27 F	AGT CAG CGC AAG TGG AAT TT
p27 R	AGT AGA ACT CGG GCA AGC TG
p53 F	AAC CGC CGA CCT ATC CTT AC
p53 R	CTT CTG TAC GGC GGT CTC TC
Rb F	AGA GAG AAC GCC ACG AAA AA
Rb R	GAT GGC TGA TCA CTT GCA GA
GAPDH F	TGT GTC CGT CGT GGA TCT GA
GAPDH R	TTG CTG TTG AAG TCG CAG GAG

Supplementary material Table S2: Primer list for ChIP (related to Figs 6,7)

Sox2-5' UTR F	CCC ATT TAT TCC CTG ACA GC
Sox2-5' UTR R	TGT GAT TAG TTT TTG GAA AGG
Sox2-SRR2 F	ATT TAT TCA GTT CCC AGT CCA AGC
Sox2-SRR2 R	CCC TCT CCC CCC ACG C
Nanog-promoter F	CAA CTT ACT AAG GTA GCC CGA GTC TTA A
Nanog-promoter R	CCT CCA AAA GTG CGG CTT T